Unfitted mixed finite element methods for elliptic interface problems

Najwa Alshehri[A1], Daniele Boffi[A,B2] and Lucia Gastaldi[C3]

[A]*Computer, electrical and mathematical sciences and engineering division, King Abdullah University of Science and Technology (KAUST), Thuwal, 23955, Saudi Arabia*
[B]*Dipartimento di Matematica 'F. Casorati', University of Pavia, I-27100 Pavia, Italy*
[C]*Dipartimento di Ingegneria Civile, Architettura, Territorio, Ambiente e di Matematica, Università degli Studi di Brescia, I-25123 Brescia, Italy*

Abstract

In this paper, new unfitted mixed finite elements are presented for elliptic interface problems with jump coefficients. Our model is based on a fictitious domain formulation with distributed Lagrange multiplier. The relevance of our investigations is better seen when applied to the framework of fluid structure interaction problems. Two finite elements schemes with piecewise constant Lagrange multiplier are proposed and their stability is proved theoretically. Numerical results compare the performance of those elements, confirming the theoretical proofs and verifying that the schemes converge with optimal rate.

Key words: Interface problems, Finite elements, Fluid-structure interactions, Discontinuous Lagrange multiplier, Fictitious domains problems, Immersed domain, Stability and inf-sup condition

1 Introduction

Elliptic interface problems with jump coefficients are important and widely used in applications including bio-science and fluid-dynamics applications.

We consider a problem where the coefficients in the governing partial differential equation may jump across the interface that separate two or more sub-domains. There are various possibilities for the decomposition of the domain. In this paper, we consider the case where one subdomain is immersed into another one. Other cases might be considered as well [13] and limiting to two subdomains doesn't affect the generality of our discussion.

To deal with interface problems, one could use fitted meshes matching at the interface as in Figure 1.A. Many existing methods are developed based on this approach such as extended finite element method [10], immersed interface method [15], multi scale finite

---

[1]E-mail: najwa.alshehri@kaust.edu.sa
[2]E-mail: daniele.boffi@kaust.edu.sa
[3]E-mail: lucia.gastaldi@unibs.it

element method [14], and many others [8, 12]. Yet, this method is challenging especially for time-dependent problems such as Fluid Structure Interaction (FSI) problems. In such problems, the mesh follows the evolution of the system which requires explicit tracking of the interface. Therefore, with large displacements and deformations, the mesh can become ill-shaped mostly around the interface. One could overcome this issue by updating the mesh at every time step which makes this approach computationally expensive and hard to use.

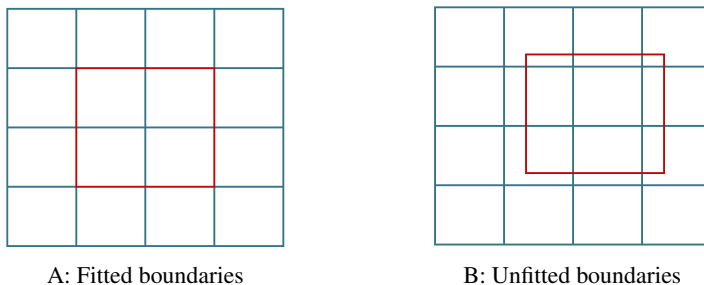A: Fitted boundaries   B: Unfitted boundaries

FIGURE 1: Fitted vs. unfitted boundaries

An alternative approach is to use unfitted meshes. In this approach, the meshes are independent of the interface which is allowed to cut through the interior of elements, see Figure 1.B. In this paper, we adapt the unfitted approach to introduce the Fictitious Domain with Distributed Lagrange Multiplier method (FD-DLM). This method is based on the Immersed Boundary Method (IBM) that was introduced by Peskin in [18] for the simulation of the blood flow in the heart in the early seventies where he approximated the solution numerically using finite differences. Later in 2003 and for the first time, the IBM was established in the framework of finite element in [4].

This reasearch led to the Fictitious Domain with Distributed Lagrange Multiplier (FD-DLM) method which has the advantage of avoiding mesh regenerations by using fixed meshes. It makes use of the so-called fictitious domain approach that was introduced in [11, 19], to fictitiously extend one mesh into the other one. Then, the two meshes are considered independent of each other and constructed only once. To this end, we add a coupling term to enforce that the solution in the extended domain coincides with the solution in the immersed domain. In our model, a Lagrange multiplier term is responsible for that.

A crucial aspect in this method is how to deal with the coupling term. Such term is represented by a bilinear form defined on suitable Hilbert spaces. For instance, in [1], the discretization of this term was represented as the scalar product of L^2. In [6] the coupling term was represented as the scalar product either in L^2 or H^1. Furthermore, the computation of the this term involves the evaluation of the integral on the immersed domain of shape functions that are supported on two different meshes. In [3] it is discussed how to implement this term in practice. It is shown that, in order to achieve optimal convergence rate of the method, one has to perform the integral exactly by examining the intersection of the two meshes. Moreover, it is observed that finding the geometric intersection cannot

be avoided even if the precision of the used quadrature rule is increased. Hence, in our numerical tests we will follow the intersection approach. More details on the coupling terms are given in Section 4.

In [1] continuous piecewise linear finite element spaces are considered for the discretization of the problem on triangular meshes. In [6] continuous piecewise bilinear finite element spaces are considered on quadrilateral meshes. Recently, [5] showed, in the framework of FSI, the stability of a linearization of the continuous problem and introduced a unified setting for the choice of the finite element spaces. This setting allows for more general choices of spaces. However, so far only continuous finite element spaces are considered for the multiplier responsible of the coupling term.

Our work is an extension to those papers where we are interested in finding stable elements with more flexibility in the choice of the multiplier. In particular, we addressed for the first time the question whether piecewise discontinuous elements can be used for the approximation of the Lagrange multiplier. The motivation of our choice originates from FSI problems, where having a discontinuous Lagrange multiplier could improve the local mass conservation properties.

In Section 2.1 we introduce in detail the problem in the continuous setting. This problem is well-posed; we then consider its discretization and propose possible choices of elements that are the main object of our study in Section 2.2. Next, we prove the well-posedness of our discrete schemes in Section 3. The stability of our schemes is based on the presence of interior degrees of freedom (so called bubble functions) in the space approximating the solution where the Lagrange multiplier is distributed. We are showing numerically in Section 4.1 that the presence of the bubble functions is necessary for the discrete inf-sup condition. Section 4.2 reports a series of numerical tests which confirm the theoretical results.

2   Formulation of the method

2.1   Model problem

Let Ω be a domain in $\mathbb{R}^d$, $d = 1, 2, 3$ with a bounded Lipschitz boundary $\partial\Omega$. We assume that Ω is subdivided into two subdomains Ω_i, $i = 1, 2$ so that $\overline{\Omega} = \overline{\Omega}_1 \cup \overline{\Omega}_2$. The subdomains are separated by a Lipschitz continuous interface $\Gamma = \overline{\Omega}_1 \cap \overline{\Omega}_2$. In order to simplify the presentation we assume that Ω_2 is immersed in Ω so that $\overline{\Gamma} \cap \partial\Omega = \emptyset$. Figure 2 reports a sketch of the situation in 2D. Then, we consider the following problem:

PROBLEM **2.1**. *Given $f_1 : \Omega_1 \to \mathbb{R}$, $f_2 : \Omega_2 \to \mathbb{R}$, find $u_1 : \Omega_1 \to \mathbb{R}$ and $u_2 : \Omega_2 \to \mathbb{R}$ such that:*

$$
\begin{align}
-\nabla \cdot (\beta_i \nabla u_i) &= f_i & \text{in } \Omega_i, \ i = 1, 2 & \quad (1a)\\
u_1 &= u_2 & \text{on } \Gamma & \quad (1b)\\
\beta_1 \nabla(u_1) \cdot \boldsymbol{n}_1 &= -\beta_2 \nabla(u_2) \cdot \boldsymbol{n}_2 & \text{on } \Gamma & \quad (1c)\\
u_1 &= 0 & \text{on } \partial\Omega_1 & \quad (1d)
\end{align}
$$

where $\boldsymbol{n}_i$, $i = 1, 2$ is the unit vector pointing out of Ω_i and normal to Γ.

This is an elliptic interface problem with jump in the coefficients and homogeneous Dirichlet boundary condition. We assume that the coefficients β_i belong to $L^\infty(\Omega_i)$ ($i = 1, 2$) and that they are bounded by below as follows:

$$\beta_1 > \underline{\beta}_1 > 0 \tag{2}$$

$$\beta_2 > \underline{\beta}_2 > 0. \tag{3}$$

In 2D, this model typically describes the displacement of a membrane made of two materials. The coefficients β_i stand for the stiffness of the materials, f_i $i = 1, 2$ for the loads applied to the membrane, and u_i for the vertical displacement in Ω_i ($i = 1, 2$), respectively. Equation (1b) guarantees the continuity of the solutions u_1 and u_2 on the interface Γ. This means that we are considering connected materials that do not break. Moreover, Equation (1c) prescribes a jump of the normal derivatives of u_1 and u_2 at the interface that is inversely proportional to the ratio of the coefficients.
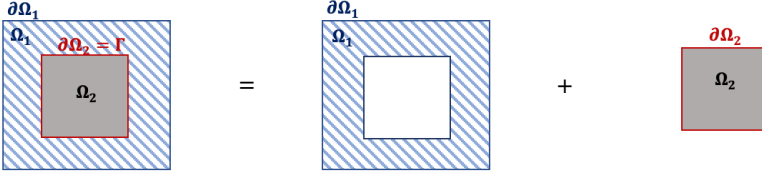

FIGURE 2: Domain decomposition in 2D.
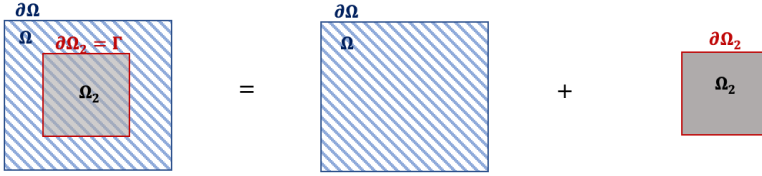
FIGURE 3: Ω_1 fictitiously extended in Ω_2 in 2D.

In this paper, we consider a fictitious domain approach, therefore we reformulate Problem 2.1 following [1] and [6]. More precisely, we extend u_1, β_1, and f_1 to Ω and denote such extensions by u, β, and f, respectively, so that $u|_{\Omega_1} = u_1$, $f|_{\Omega_1} = f_1$, and $\beta|_{\Omega_1} = \beta_1$. Moreover, we enforce the extended solution u to coincide with u_2 in Ω_2, i.e. $u|_{\Omega_2} = u_2$ by introducing a Lagrange multiplier. The resulting formulation will be called FD-DLM.

In view of the introduction of the variational formulation of the problem, we recall some notation. For any open connected domain, or part of a domain, $\omega \subset \mathbb{R}^d$ for $d = 2, 3$, we denote the standard Lebesgue and Sobolev spaces by $L^2(\omega)$ and $H^1(\omega)$, respectively. Those spaces are endowed with their norms; $\|\cdot\|_{L^2(\omega)} = \|\cdot\|_{0,\omega}$ and $\|\cdot\|_{H^1(\omega)} = \|\cdot\|_{1,\omega}$. Moreover, $(\cdot, \cdot)_\omega$ stands for the scalar product in $L^2(\omega)$.

Let us consider the spaces

$$V = H_0^1(\Omega) = \left\{ v \in H^1(\Omega) \mid v = 0 \text{ on } \partial\Omega \right\}$$
$$V_2 = H^1(\Omega_2)$$

endowed with their natural norms $\|v\|_V = |v|_{1,\Omega} = \|\nabla v\|_{0,\Omega}$ and $\|v_2\|_{V_2} = \|v_2\|_{1,\Omega_2}$, respectively.

We denote by Λ the dual space of V_2, i.e. $\Lambda = \left[H^1(\Omega_2) \right]^*$, endowed with the following dual norm:

$$\|\mu\|_\Lambda = \sup_{v_2 \in V_2} \frac{\langle \mu, v_2 \rangle}{\|v_2\|_{V_2}}$$

where $\langle \cdot, \cdot \rangle$ is the duality paring between V_2 and its dual space Λ.

In [1] it has been proved that Problem 2.1 is equivalent to the following fictitious domain formulation with distributed Lagrange multiplier.

PROBLEM **2.2**. *Given $f \in L^2(\Omega)$, $f_2 \in L^2(\Omega_2)$, $\beta \in L^\infty(\Omega)$ and $\beta_2 \in L^\infty(\Omega_2)$ with $f|_{\Omega_1} = f_1$ and $\beta|_{\Omega_1} = \beta_1$, find $(u, u_2, \lambda) \in V \times V_2 \times \Lambda$ such that*

$$\begin{aligned}
(\beta\nabla u, \nabla v)_\Omega + \langle \lambda, v|_{\Omega_2} \rangle &= (f, v)_\Omega && \forall v \in V \\
((\beta_2 - \beta)\nabla u_2, \nabla v_2)_{\Omega_2} - \langle \lambda, v_2 \rangle &= (f_2 - f, v_2)_{\Omega_2} && \forall v_2 \in V_2 \\
\langle \mu, u|_{\Omega_2} - u_2 \rangle &= 0 && \forall \mu \in \Lambda.
\end{aligned}$$

After some standard calculations, one can obtain the following characterization of λ, that will be useful to estimate the approximation error, see [1]:

$$\langle \lambda, v_2 \rangle = - \int_{\Omega_2} \left(\frac{\beta}{\beta_2} f_2 - f \right) v_2 \, dx + \int_\Gamma (\beta_2 - \beta)\nabla u_2 \cdot \mathbf{n}_2 \, v_2 \, d\gamma. \tag{4}$$

Clearly, Problem 2.2 is a saddle point problem which can be written in operator form as follow:

$$\begin{pmatrix} A_1 & 0 & C_1^T \\ 0 & A_2 & -C_2^T \\ C_1 & -C_2 & 0 \end{pmatrix} \begin{pmatrix} u \\ u_2 \\ \lambda \end{pmatrix} = \begin{pmatrix} F_1 \\ F_2 \\ 0 \end{pmatrix}, \tag{5}$$

where A_1 and A_2 are the operators associated with the bilinear forms $(\beta\nabla u, \nabla v)_\Omega$ and $((\beta_2 - \beta)\nabla u_2, \nabla v_2)_{\Omega_2}$, respectively. Moreover, $(C_1, -C_2)$ is the operator pair that is associated with the bilinear form $\langle \mu, u|_{\Omega_2} - u_2 \rangle$ with kernel:

$$\mathbb{K} = \left\{ (u, u_2) \in V \times V_2 : \langle \mu, u|_{\Omega_2} - u_2 \rangle = 0, \forall \mu \in \Lambda \right\}.$$

Notice that due to the definition of Λ we have that $u|_{\Omega_2} = u_2$ for all $(u, u_2) \in \mathbb{K}$.

Typically, in order to prove the well-posedness of a continuous saddle point problem like Problem 2.2, one needs to verify the following two sufficient conditions (see [2]).

- **Continuous elker condition:** There exists a constant $\overline{\gamma_1} > 0$ such that for all

(v, v_2) in $\mathbb{K}$ the following inequality holds true

$$(\beta \, \nabla v, \nabla v)_\Omega + ((\beta_2 - \beta) \, \nabla v_2, \nabla v_2)_{\Omega_2} \geq \overline{\gamma_1} \left(\|v\|_V^2 + \|v_2\|_{V_2}^2 \right).$$

- **Continuous inf-sup condition:** There exists a constant $\overline{\gamma_2} > 0$, such that for all $\mu \in \Lambda$ the following bound holds true

$$\sup_{(v, v_2) \in V \times V_2} \frac{\langle \mu, v|_{\Omega_2} - v_2 \rangle}{\left(\|v\|_V^2 + \|v_2\|_{V_2}^2 \right)^{\frac{1}{2}}} \geq \overline{\gamma_2} \, \|\mu\|_\Lambda.$$

Both conditions were shown to hold in [1]. Therefore, a unique stable solution exists for Problem 2.2 and we can state the following proposition (see [2]).

PROPOSITION **2.1** (**Stability**). *Given $f \in L^2(\Omega)$ and $f_2 \in L^2(\Omega_2)$, there exists a unique solution (u, u_2, λ) in $V \times V_2 \times \Lambda$ for Problem 2.2 which satisfies the following a priori estimate:*

$$\|u\|_V + \|u_2\|_{V_2} + \|\lambda\|_\Lambda \leq C \left(\|f\|_{0,\Omega} + \|f_2\|_{0,\Omega_2} \right).$$

REMARK **1**. *It is known that the regularity of the solution (u_1, u_2) of an elliptic interface problem with discontinuous coefficients and a Lipschitz interface Γ, such as Problem 2.1, is limited by the presence of re-entrant corners of the interface and of the external boundary. Hence we have that there exists s with $\frac{3}{2} < s \leq 2$ such that $u_i \in H^s(\Omega_i)$ for $i = 1, 2$, (see [17]). Moreover, since the solution $u \in H_0^1(\Omega)$ of Problem 2.2 exhibits jumps in the derivative normal to the interface, it belongs to $H^r(\Omega)$, with $1 < r < \frac{3}{2}$.*

2.2 Finite element discretization

Let $\mathcal{T}$ and $\mathcal{T}_2$ be two shape-regular meshes of the fictitiously extended domain Ω and the immersed domain Ω_2, respectively. Here, we are considering quadrilateral meshes in 2D and hexahedral in 3D, with h and h_2 denoting the maximum mesh size of $\mathcal{T}$ and $\mathcal{T}_2$, respectively. We introduce the finite element spaces $V_h \subset V$, $V_{2h} \subset V_2$, and $\Lambda_h \subset \Lambda$. V_h and V_{2h} contain piecewise polynomials continuous across the interelement boundaries, while for Λ_h we choose discontinuous finite elements. However, since $\Lambda_h \subset L^2(\Omega_2)$, the duality paring in Problem 2.2 can be evaluated using the L^2 scalar product in Ω_2. Then, the discrete version of Problem 2.2 reads:

PROBLEM **2.3**. *Given $f \in L^2(\Omega)$ and $f_2 \in L^2(\Omega_2)$, find $(u_h, u_{2h}, \lambda_h) \in V_h \times V_{2h} \times \Lambda_h$ such that*

$$\begin{aligned}
(\beta \nabla u_h, \nabla v_h)_\Omega + (\lambda_h, v_h|_{\Omega_2})_{\Omega_2} &= (f, v_h)_\Omega &\forall v_h \in V_h \\
((\beta_2 - \beta) \nabla u_{2h}, \nabla v_{2h})_{\Omega_2} - (\lambda_h, v_{2h})_{\Omega_2} &= (f_2 - f, v_{2h})_{\Omega_2} &\forall v_{2h} \in V_{2h} \\
(\mu_h, u_h|_{\Omega_2} - u_{2h})_{\Omega_2} &= 0 &\forall \mu_h \in \Lambda_h.
\end{aligned}$$

For K an element of $\mathcal{T}$ or $\mathcal{T}_2$, we define $Q_k(K)$, $k \geq 1$, to be the space of finite elements that are polynomials of degree at most k, separately in each variable on K. If $k = 0$ then $Q_0(K)$ is the space of constant polynomials and will be denoted by $P_0(K)$.

Moreover, let $B(K) \in Q_2(K)$ be a bubble function defined on K and vanishing at the boundary of the element K. This function will be used in this work to enrich the space $Q_1(K)$.

In the following we are going to discretize the Lagrange multiplier by piecewise constants, hence we introduce the following natural choices for $V_h \times V_{2h} \times \Lambda_h$.

- **Element 1:** $Q_1 - (Q_1 + B) - P_0$
  In this element we define the discrete subspaces V_h, V_{2h}, Λ_h to be

$$V_h = \{v_h \in V : v_h|_K \in Q_1(K), \forall K \in \mathcal{T}\}$$
$$V_{2h} = \{v_{2h} \in V_2 : v_{2h}|_K \in Q_1(K) + B(K), \forall K \in \mathcal{T}_2\} \tag{6}$$
$$\Lambda_h = \{\mu_h \in \Lambda : \mu_h|_K \in P_0(K), \forall K \in \mathcal{T}_2\}.$$

  Hence, the solution u_h is approximated by piecewise bilinear polynomials and u_{2h} by piecewise bilinear polynomials enriched by bubble functions, so that, five degrees of freedom are used per element in the space V_{2h} (see Figure 4).

- **Element 2:** $Q_2 - Q_2 - P_0$
  Here, we define the discrete subspaces V_h, V_{2h}, Λ_h to be

$$V_h = \{v_h \in V : v_h|_K \in Q_2(K), \forall K \in \mathcal{T}\}$$
$$V_{2h} = \{v_{2h} \in V_2 : v_{2h}|_K \in Q_2(K), \forall K \in \mathcal{T}_2\} \tag{7}$$
$$\Lambda_h = \{\mu_h \in \Lambda : \mu_h|_K \in P_0(K), \forall K \in \mathcal{T}_2\}$$

  where we approximate both u_h, u_{2h} by piecewise biquadratic polynomials. Hence, we use nine nodes for each element in the spaces V_h and V_{2h} (see Figure 5). It is clear that comparing with Element 1, V_{2h} uses four extra nodes at the middle of each edge, while V_h requires five extra degrees of freedoms, so this element is computationally more expensive than Element 1.
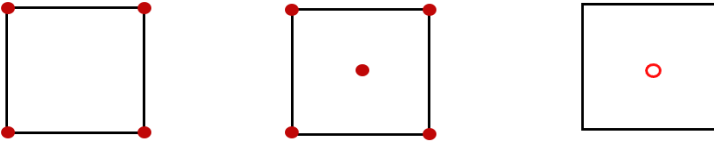
FIGURE 4: Element 1 in 2D , $Q_1 - (Q_1 + B) - P_0$.
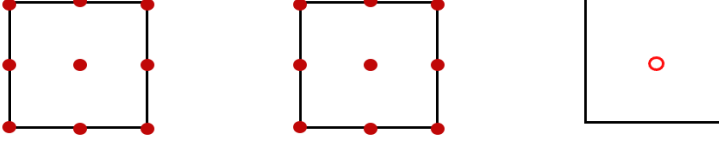
FIGURE 5: Element 2 in 2D, $Q_2 - Q_2 - P_0$.

3 Error estimate

In this section, we study the existence of a unique stable solution of Problem 2.3. Since it is a discrete saddle point problem, sufficient conditions for its well-posedness are the discrete elker and inf-sup conditions (see [2]).

Let the discrete kernel $\mathbb{K}_h$ associated with the bilinear form $(\mu_h, u_h|_{\Omega_2} - u_{2h})_{\Omega_2}$ be defined as follow:

$$\mathbb{K}_h = \{(u_h, u_{2h}) \in V_h \times V_{2h} : (\mu_h, u_h|_{\Omega_2} - u_{2h})_{\Omega_2} = 0, \forall \mu_h \in \Lambda_h\}$$

Then, the following proposition states the discrete elker condition.

PROPOSITION **3.1** (**Discrete elker condition**). *Let us consider V_h, V_{2h}, Λ_h defined in (6) and (7) and assume that the coefficients satisfy $\beta_2 > \beta > \underline{\beta} > 0$ in Ω_2, then there exists a constant $\gamma_1 > 0$ independent of the discretization parameters h, h_2, such that for all $(v_h, v_{2h}) \in \mathbb{K}_h$ the following inequality holds true.*

$$(\beta \nabla v_h, \nabla v_h)_\Omega + ((\beta_2 - \beta)\nabla v_{2h}, \nabla v_{2h})_{\Omega_2} \geq \gamma_1 \left[\|v_h\|_V^2 + \|v_{2h}\|_{V_2}^2 \right].$$

Proof. For all $(v_h, v_{2h}) \in \mathbb{K}_h$ we have:

$$(\beta \nabla v_h, \nabla v_h)_\Omega + ((\beta_2 - \beta)\nabla v_{2h}, \nabla v_{2h})_{\Omega_2} = \beta \|\nabla v_h\|_{0,\Omega}^2 + (\beta_2 - \beta) \|\nabla v_{2h}\|_{0,\Omega_2}^2$$
$$\geq \underline{\beta} \|\nabla v_h\|_{0,\Omega}^2 + \eta_0 \|\nabla v_{2h}\|_{0,\Omega_2}^2,$$

where η_0 is such that $\beta_2 - \beta \geq \eta_0 > 0$.

Since $V = H_0^1(\Omega)$, we can apply the Poincaré inequality $\|v_h\|_{0,\Omega} \leq C_\Omega \|\nabla v_h\|_{0,\Omega}$, and we have that:

$$(\beta \nabla v_h, \nabla v_h)_\Omega \geq \frac{\underline{\beta}}{2} \left(1 + \frac{1}{C_\Omega^2}\right) \|v_h\|_{1,\Omega}^2.$$

It remains to bound by below $\|\nabla v_{2h}\|_{0,\Omega_2}$ by means of $\|v_{2h}\|_{1,\Omega_2}$. In order to use the Poincaré–Wirtinger inequality, we split v_{2h} as follows

$$v_{2h} = E(v_{2h}) + \left[v_{2h} - E(v_{2h})\right]$$

where $E(v_{2h}) \in \mathbb{R}$ is the mean value of v_{2h}. Then,

$$\|v_{2h}\|_{0,\Omega_2} \leq \|E(v_{2h})\|_{0,\Omega_2} + \|v_{2h} - E(v_{2h})\|_{0,\Omega_2}$$
$$\leq \|E(v_{2h})\|_{0,\Omega_2} + C \|\nabla v_{2h}\|_{0,\Omega_2}$$

Now, since $(v_h, v_{2h}) \in \mathbb{K}_h$, and Λ_h contains constant functions on Ω_2, we have

$$(E(v_{2h}), E(v_{2h}))_{\Omega_2} = (E(v_{2h}), v_{2h})_{\Omega_2} - (E(v_{2h}), v_{2h} - E(v_{2h}))_{\Omega_2}$$
$$= (E(v_{2h}), v_h|_{\Omega_2})_{\Omega_2} - (E(v_{2h}), v_{2h} - E(v_{2h}))_{\Omega_2} \qquad (8)$$
$$= (E(v_{2h}), v_h|_{\Omega_2})_{\Omega_2}$$

Then, (8) gives the bound

$$\|E(v_{2h})\|_{0,\Omega_2}^2 \leq \|E(v_{2h})\|_{0,\Omega_2} \|v_h\|_{0,\Omega_2}$$

Hence,

$$\|E(v_{2h})\|_{0,\Omega_2} \leq \|v_h\|_{0,\Omega_2}$$

which conclude the proof.

$\diamondsuit$

REMARK **2**. *In a particular case and under the additional condition that h_2/h^d is sufficiently small, in [6] it has been shown that the discrete elker condition holds true even if the constraint $\beta_2 > \beta$ is not verified. In that case triangular linear elements were used for the approximation of both V_2 and Λ.*

In the next proposition, we prove the discrete inf-sup condition.

PROPOSITION **3.2** (**Discrete inf-sup condition**). *Let V_h, V_{2h}, Λ_h be the spaces defined in* (6) *and* (7) *for Element 1 and Element 2, respectively. Then there exists a positive constant $\gamma_2 > 0$ independent of the discretization parameters h, h_2, such that the following discrete inf-sup condition holds.*

$$\sup_{(v_h, v_{2h}) \in V_h \times V_{2h}} \frac{(\mu_h, v_h|_{\Omega_2} - v_{2h})_{\Omega_2}}{\left(\|v_h\|_V^2 + \|v_{2h}\|_{V_2}^2\right)^{\frac{1}{2}}} \geq \gamma_2 \|\mu_h\|_\Lambda . \qquad (9)$$

Proof. We prove this proposition for Element 1. The same proof carries on for Element 2.
Since $v_h = 0$ is a possible choice in V_h, we have that

$$\sup_{(v_h, v_{2h}) \in V_h \times V_{2h}} \frac{(\mu_h, v_h|_{\Omega_2} - v_{2h})_{\Omega_2}}{\left(\|v_h\|_V^2 + \|v_{2h}\|_{V_2}^2\right)^{\frac{1}{2}}} \geq \sup_{v_{2h} \in V_{2h}} \frac{(\mu_h, v_{2h})_{\Omega_2}}{\|v_{2h}\|_{V_2}} .$$

Hence, it is enough to prove the following bound:

$$\sup_{v_{2h} \in V_{2h}} \frac{(\mu_h, v_{2h})_{\Omega_2}}{\|v_{2h}\|_{V_2}} \geq \gamma_2 \|\mu_h\|_\Lambda . \qquad (10)$$

In order to show that (10) is satisfied, we use a Fortin trick (see [7, Prop. 5.4.2]). Due to the fact that the continuous inf-sup condition is satisfied, the aim of this proof is to

find a linear Fortin operator $\Pi_h : V_2 \to V_{2h}$ that satisfies the following relations for all $v_2 \in V_2$:

$$\begin{aligned}
&\text{i) } \|\Pi_h v_2\|_{V_2} \leq C \|v_2\|_{V_2} \\
&\text{ii) } (\mu_h, v_2)_{\Omega_2} = (\mu_h, \Pi_h v_2)_{\Omega_2} \quad \forall \mu_h \in \Lambda_h.
\end{aligned} \tag{11}$$

We introduce the following subspaces of V_{2h}:

$$\overline{\overline{V_{2h}}} = \{v_{2h} \in V_2 : v_{2h}|_K \in Q_1(K), \forall K \in \mathcal{T}_2\} \subset V_{2h}$$

$$\overline{V_{2h}} = \{v_{2h} \in V_2 : v_{2h}|_K \in B(K), \forall K \in \mathcal{T}_2\} \subset V_{2h}$$

Let $\Pi_h = \Pi_1 + \Pi_2(I - \Pi_1)$ where $\Pi_1 : V_2 \to \overline{\overline{V_{2h}}} \subset V_{2h}$ is the Clément's operator, such that for all $v_2 \in V_2$

$$\sum_{K \in \mathcal{T}_2} h_K^{-2} \|v_2 - \Pi_1 v_2\|_{0,K}^2 \leq C \|v_2\|_{V_2}^2 \tag{12a}$$

$$\sum_{K \in \mathcal{T}_2} \|v_2 - \Pi_1 v_2\|_{1,K}^2 \leq C \|v_2\|_{V_2}^2 \tag{12b}$$

and $\Pi_2 : V_2 \to \overline{V_{2h}} \subset V_{2h}$ such that $\Pi_2(p_i) = 0$ for all nodes p_i at vertices of the element $K \in \mathcal{T}_2$ and

$$\int_K \Pi_2 v_2 = \int_K v_2 \qquad\qquad \forall v_2 \in V_2 \text{ and } K \in \mathcal{T}_2 \tag{13}$$

Let $\mathcal{F}_K^{-1}$ be the affine mapping that maps objects from the current element, $K \in \mathcal{T}_2$, to the reference element denoted by $\hat{K}$, that is the unit square in 2D and the unit cube in 3D. Then, $\hat{v}_2 = v_2 \circ \mathcal{F}_K$ where symbols with hat refer to quantities evaluated in the reference domain $\hat{K}$.

Let $|K|$ be the measure of the element K. Then,

$$\int_{\hat{K}} \widehat{\Pi_2 v_2} = |K|^{-1} \int_K \Pi_2 v_2 = |K|^{-1} \int_K v_2 = |K|^{-1} |K| \int_{\hat{K}} \hat{v}_2 = \int_{\hat{K}} \hat{v}_2$$

which means that $\widehat{\Pi_2}$ also satisfies equation (13). Moreover, let us define the following:

$$\left\| \left\| \widehat{\Pi_2 v_2} \right\| \right\| = \left| \int_{\hat{K}} \widehat{\Pi_2 v_2} \right|$$

It is clear that this is a norm in this specific case, since the function $\widehat{\Pi_2 v_2}$ by definition is the bubble in the reference element. Hence, $\left| \int_{\hat{K}} \widehat{\Pi_2 v_2} \right| = 0$ if and only if $\widehat{\Pi_2 v_2} = 0$. Using the definition of Π_h and the equality in (13), we get

$$(\mu_h, v_2 - \Pi_h v_2)_{\Omega_2} = (\mu_h, (v_2 - \Pi_1 v_2) - \Pi_2(v_2 - \Pi_1 v_2))_{\Omega_2} = 0 \quad \forall \mu_h \in \Lambda_h$$

which proves that the proposed operator Π_h satisfies condition ii) in (11).

Now, we need to show condition i) for all $v_2 \in V_2$, that is:

$$\|\Pi_h v_2\|_{V_2} = \|\Pi_1 v_2 + \Pi_2(v_2 - \Pi_1 v_2)\|_{V_2} \leq C \|v_2\|_{V_2} . \tag{14}$$

It is clear that (12b) implies

$$\|\Pi_1 v_2\|_{V_2} \leq C \|v_2\|_{V_2}.$$ (15)

For the sake of simplicity, let $w = v_2 - \Pi_1 v_2$ and write the H^1-norm as follows:

$$\|\Pi_2 w\|_{1,\Omega_2}^2 = \|\Pi_2 w\|_{0,\Omega_2}^2 + |\Pi_2 w|_{1,\Omega_2}^2$$ (16)

For all $K \in \mathcal{T}_2$, we estimate the first term in (16) as follows:

$$
\begin{aligned}
\|\Pi_2 w\|_{0,K} &\leq C \, |K|^{\frac{1}{2}} \left\|\widehat{\Pi_2 w}\right\|_{0,\hat{K}} && \textit{mapping to the reference element } \hat{K} \\
&\leq C \, |K|^{\frac{1}{2}} \left|\int_{\hat{K}} \widehat{\Pi_2 w}\right| && \textit{by equivalence of norms in finite dimensions} \\
&= C \, |K|^{\frac{1}{2}} \left|\int_{\hat{K}} \hat{w}\right| && \textit{since } \widehat{\Pi_2} \textit{ satisfies (13)} \\
&\leq C \, |K|^{\frac{1}{2}} \|\hat{w}\|_{0,\hat{K}} && \textit{by Cauchy-Schwarz inequality} \\
&\leq C \, |K|^{\frac{1}{2}} |K|^{-\frac{1}{2}} \|w\|_{0,K} && \textit{mapping back to the physical element } K \\
&= C \, \|w\|_{0,K}
\end{aligned}
$$

Similarly, using the same argument as before we have

$$
\begin{aligned}
\|\nabla \Pi_2 w\|_{0,K} &\leq C \, h_K^{-1} \, |K|^{\frac{1}{2}} \left|\widehat{\Pi_2 w}\right|_{1,\hat{K}} \leq C \, h_K^{-1} \, |K|^{\frac{1}{2}} \left|\int_{\hat{K}} \widehat{\Pi_2 w}\right| \\
&\leq C \, h_K^{-1} \, |K|^{\frac{1}{2}} \left|\int_{\hat{K}} \hat{w}\right| \leq C \, h_K^{-1} \, |K|^{\frac{1}{2}} \|\hat{w}\|_{0,\hat{K}}.
\end{aligned}
$$

Mapping back to the current element K, we obtain:

$$\|\nabla \Pi_2 w\|_{0,K} \leq C \, h_K^{-1} \, |K|^{\frac{1}{2}} \, |K|^{-\frac{1}{2}} \|w\|_{0,K} = C \, h_K^{-1} \|w\|_{0,K}.$$ (17)

By substituting (17) in (16) and using the bounds of Π_1 in (12a), we get

$$\|\Pi_2(v_2 - \Pi_1 v_2)\|_{V_2}^2 \leq C \sum_{K \in \mathcal{T}_2} h_K^{-2} \|v_2 - \Pi_1 v_2\|_{0,K}^2 \leq C \|v_2\|_{V_2}^2.$$ (18)

Using the triangle inequality, and applying the results of (15) and (18), yield that condition i) holds, in fact

$$
\begin{aligned}
\|\Pi_h v_2\|_{V_2} &= \|\Pi_1 v_2 + \Pi_2(v_2 - \Pi_1 v_2)\|_{V_2} \\
&\leq \|\Pi_1 v_2\|_{V_2} + \|\Pi_2(v_2 - \Pi_1 v_2)\|_{V_2} \\
&\leq C \|v_2\|_{V_2}.
\end{aligned}
$$

This concludes the proof and shows that the H^1- stability of the constructed Fortin operator Π_h is satisfied. Therefore, the discrete inf-sup condition (9) holds. $\diamond$

REMARK **3**. *Proposition 3.2 shows rigorously that the inf-sup condition for Element 1 and Element 2 is satisfied uniformly. The bubble function in the space V_{2h} is necessary for the stability of the element. In fact, in Section 4.1 we give numerical evidence that we*

do not have a uniform inf-sup bound if we modify Element 1 and remove the bubble to become $Q_1 - Q_1 - P_0$.

Thanks to Propositions 3.1 and 3.2 there exists a unique stable solution (u_h, u_{2h}, λ_h) for Problem 2.3 in the spaces $V_h \times V_{2h} \times \Lambda_h$ that are defined in (6) and (7). Moreover, by taking into consideration the regularity results of the solutions u and u_2 recalled in Remark 1, we can state the following a priori error estimate.

PROPOSITION **3.3** (**Error estimate**). *Given* $(f, f_2) \in L^2(\Omega) \times L^2(\Omega_2)$. *Let* $(u, u_2, \lambda) \in V \times V_2 \times \Lambda$ *and* $(u_h, u_{2h}, \lambda_h) \in V_h \times V_{2h} \times \Lambda_h$ *be the solutions of Problem 2.2 and Problem 2.3, respectively. We consider Element 1 and Element 2 defined in* (6) *and* (7). *Then, under the assumption that the mesh* $\mathcal{T}_2$ *is quasi uniform, the following error estimate holds true:*

$$\|u - u_h\|_V + \|u_2 - u_{2h}\|_{V_2} + \|\lambda - \lambda_h\|_\Lambda$$
$$\leq C \left(h^{r-1} \|u\|_{r,\Omega} + \max(h_2^{s-1}, h_2^{1-t}) \|u_2\|_{s,\Omega_2} + h_2 \left\| \frac{\beta}{\beta_2} f_2 - f \right\|_{0,\Omega_2} \right)$$

with $1 < r < 3/2$ *and* $3/2 < s \leq 2$, *defined in Remark 1, and for* $1/2 < t < 1$.

Proof. Thanks to the continuous elker and inf-sup conditions and their discrete version in Propositions 3.1 and 3.2, the theory of saddle point problem yields the usual quasi-optimal error estimate (see [2, Th. 5.2.2]), that in this case, reads as follows

$$\|u - u_h\|_V + \|u_2 - u_{2h}\|_{V_2} + \|\lambda - \lambda_h\|_\Lambda$$
$$\leq C \left(\inf_{v \in V_h} \|u - v\|_V + \inf_{v_2 \in V_{2h}} \|u_2 - v_2\|_{V_2} + \inf_{\mu \in \Lambda_h} \|\lambda - \mu\|_\Lambda \right).$$

As a consequence of the regularity of u and u_2 reported in Remark 1, standard arguments on the approximation error for the spaces V_h and V_{2h} imply that

$$\inf_{v \in V_h} \|u - v\|_V \leq Ch^{r-1}|u|_{r,\Omega}$$
$$\inf_{v_2 \in V_{2h}} \|u_2 - v_2\|_{V_2} \leq Ch_2^{s-1}|u_2|_{s,\Omega_2}.$$

The estimate of the best approximation of λ requires a more careful analysis. A similar consideration has been performed in [1, Prop. 6] in a different setting. Actually, taking into account (4), the Lagrange multiplier can be represented as the sum of two pieces $\lambda = \lambda_1 + \lambda_2$ with

$$\langle \lambda_1, v_2 \rangle = \int_{\Omega_2} ((\beta/\beta_2)f_2 - f)v_2 \, dx$$
$$\langle \lambda_2, v_2 \rangle = \int_\Gamma (\beta_2 - \beta)\nabla u_2 \cdot \mathbf{n}_2 v_2 \, d\gamma. \tag{19}$$

We treat separately the two pieces and look for two elements in Λ_h which approximate λ_1 and λ_2.

Since $f \in L^2(\Omega)$, $f_2 \in L^2(\Omega_2)$ and since we assumed the bound (2), the first equality in (19) implies that $\lambda_1 \in L^2(\Omega_2)$ with $\|\lambda_1\|_{0,\Omega_2} \leq \|(\beta/\beta_2)f_2 - f\|_{0,\Omega_2}$. Let

$P_0 : L^2(\Omega_2) \to \Lambda_h$ be the L^2-projection onto Λ_h, we set $\lambda_{1h} = P_0\lambda_1 \in \Lambda_h$ with

$$(\lambda_1 - \lambda_{1h}, \mu_h) = 0 \quad \forall \mu_h \in \Lambda_h.$$

Then we observe that

$$\|\lambda_1 - \lambda_{1h}\|_\Lambda = \sup_{v_2 \in V_2} \frac{\langle \lambda_1 - \lambda_{1h}, v_2\rangle}{\|v_2\|_{V_2}} = \sup_{v_2 \in V_2} \frac{(\lambda_1 - \lambda_{1h}, v_2)}{\|v_2\|_{V_2}},$$

but

$$(\lambda_1 - \lambda_{1h}, v_2) = (\lambda_1 - \lambda_{1h}, v_2 - P_0 v_2) = (\lambda_1, v_2 - P_0 v_2)$$
$$\leq \|\lambda_1\|_{0,\Omega_2} \|v_2 - P_0 v_2\|_{0,\Omega_2} \leq C \|(\beta/\beta_2)f_2 - f\|_{0,\Omega_2} h_2 \|v_2\|_{V_2}.$$

Therefore we end up with

$$\|\lambda_1 - \lambda_{1h}\|_\Lambda \leq C h_2 \|(\beta/\beta_2)f_2 - f\|_{0,\Omega_2}. \tag{20}$$

Let us now construct an approximation of λ_2 and bound the approximation error. Remark 1 states that $u_2 \in H^s(\Omega_2)$ for $3/2 < s \leq 2$. Therefore the trace of the normal derivative of u_2 belongs to $H^{s-3/2}(\Gamma)$ and we can infer from the second equality in (19) that $\lambda_2 \in H^{-t}(\Omega_2)$ with $1/2 < t < 1$, namely by trace inequality we have

$$\|\lambda_2\|_{H^{-t}(\Omega_2)} = \sup_{v_2 \in H^t(\Omega_2)} \frac{\langle \lambda_2, v_2\rangle}{\|v_2\|_{H^t(\Omega_2)}} = \sup_{v_2 \in H^t(\Omega_2)} \frac{\int_\Gamma (\beta_2 - \beta)\nabla u_2 \cdot \mathbf{n}_2 v_2 \, d\gamma}{\|v_2\|_{H^t(\Omega_2)}}$$
$$\leq \sup_{v_2 \in H^t(\Omega_2)} \frac{\|\nabla u_2 \cdot \mathbf{n}_2\|_{H^{s-3/2}(\Gamma)} \|v_2\|_{H^{3/2-s}(\Gamma)}}{\|v_2\|_{H^t(\Omega_2)}}$$
$$\leq C \sup_{v_2 \in H^t(\Omega_2)} \frac{\|u_2\|_{H^s(\Omega_2)} \|v_2\|_{H^{t-1/2}(\Gamma)}}{\|v_2\|_{H^t(\Omega_2)}}$$
$$\leq C \sup_{v_2 \in H^t(\Omega_2)} \frac{\|u_2\|_{H^s(\Omega_2)} \|v_2\|_{H^t(\Omega_2)}}{\|v_2\|_{H^t(\Omega_2)}} = C \|u_2\|_{H^s(\Omega_2)}.$$

Let $\lambda_{2h} \in \Lambda_h$ be such that

$$\langle \lambda_{2h}, v_{2h}\rangle = \int_\Gamma (\beta_2 - \beta)\nabla u_2 \cdot \mathbf{n}_2 v_{2h} \, d\gamma \quad \forall v_{2h} \in V_{2h}$$

then it is easily seen that $\langle \lambda_2 - \lambda_{2h}, v_{2h}\rangle = 0$ for all $v_{2h} \in V_{2h}$ so that we have for $v_{2h} \in V_{2h}$

$$\langle \lambda_2 - \lambda_{2h}, v_2\rangle = \langle \lambda_2 - \lambda_{2h}, v_2 - v_{2h}\rangle = \langle \lambda_2, v_2 - v_{2h}\rangle - (\lambda_{2h}, v_2 - v_{2h}). \tag{21}$$

Using (19), we can apply trace inequalities and standard approximation results in V_{2h} to

achieve the following estimate:

$$
\begin{aligned}
\langle \lambda_2, v_2 - v_{2h} \rangle &= \int_\Gamma (\beta_2 - \beta) \nabla u_2 \cdot \mathbf{n}_2 (v_2 - v_{2h}) \, d\gamma \\
&\leq \|\nabla u_2 \cdot \mathbf{n}_2\|_{H^{s-3/2}(\Gamma)} \|v_2 - v_{2h}\|_{H^{3/2-s}(\Gamma)} \\
&\leq C \|u_2\|_{H^s(\Omega_2)} \, h_2^{s-1} \|v_2\|_{H^{1/2}(\Gamma)} \\
&\leq C h_2^{s-1} \|u_2\|_{H^s(\Omega_2)} \|v_2\|_{H^1(\Omega_2)} .
\end{aligned}
$$

It remains to bound the second term in (21): we have

$$
(\lambda_{2h}, v_2 - v_{2h}) \leq \|\lambda_{2h}\|_{0,\Omega_2} \|v_2 - v_{2h}\|_{0,\Omega_2} \leq C h_2 \|\lambda_{2h}\|_{0,\Omega_2} \|v_2\|_{1,\Omega_2}
$$

In order to conclude the proof, we now estimate $\|\lambda_{2h}\|_{0,\Omega_2}$. Recalling the Fortin operator Π_h satisfying (11), we have

$$
\begin{aligned}
\|\lambda_{2h}\|_{0,\Omega_2} &= \sup_{v_2 \in V_2} \frac{\langle \lambda_{2h}, v_2 \rangle}{\|v_2\|_{0,\Omega_2}} = \sup_{v_2 \in V_2} \frac{\langle \lambda_{2h}, \Pi_h v_2 \rangle}{\|v_2\|_{0,\Omega_2}} = \sup_{v_2 \in V_2} \frac{\langle \lambda_2, \Pi_h v_2 \rangle}{\|v_2\|_{0,\Omega_2}} \\
&\leq \sup_{v_2 \in V_2} \frac{\|\lambda_2\|_{H^{-t}(\Omega_2)} \|\Pi_h v_2\|_{H^t(\Omega_2)}}{\|v_2\|_{0,\Omega_2}} \\
&\leq C h_2^{-t} \|u_2\|_{H^s(\Omega_2)} \sup_{v_2 \in V_2} \frac{\|\Pi_h v_2\|_{0,\Omega_2}}{\|v_2\|_{0,\Omega_2}}
\end{aligned}
$$

The last supremum can be bounded if we provide a uniform $L^2(\Omega_2)$ estimate of the Fortin operator. Looking at the construction of the Fortin operator as $\Pi_h v_2 = \Pi_1 v_2 + \Pi_2(v_2 - \Pi_1 v_2)$, and inspecting the proof of its stability, it turns out that this can be done if we replace the Clément interpolation Π_1 with an interpolation which is bounded in $L^2(\Omega_2)$. This can be done by adopting the quasi-interpolation operator introduced in [9], denoted again Π_1 for simplicity, and which has been proved to have the required stability

$$
\|\Pi_1 v_2\|_{0,\Omega_2} \leq C \|v_2\|_{0,\Omega_2}.
$$

We finally get

$$
(\lambda_{2h}, v_2 - v_{2h}) \leq C h_2 \|\lambda_{2h}\|_{0,\Omega_2} \|v_2\|_{1,\Omega_2} \leq C h_2^{1-t} \|u_2\|_{H^s(\Omega_2)} \|v_2\|_{H^1(\Omega_2)}.
$$

Putting together all the pieces we see that the best approximations of u, u_2, and λ converge with order h^{r-1}, h_2^{s-1}, and h_2^{1-t}, respectively. In the case when $h_2 < 1$, since $s - 1 > 1 - t$, we get that h_2^{s-1} is dominated by h_2^{1-t}. Therefore, the final rate of convergence is given by the maximum between h^{r-1} and h_2^{1-t}. $\diamond$

REMARK **4**. *This paper only considers quadrilateral and hexahedra meshes. However, all results and proofs might be easily extended to triangular and tetrahedra meshes with the corresponding element choices $P_1 - (P_1 + \overline{B}) - P_0$ and $P_2 - (P_2 + \overline{B}) - P_0$ where $\overline{B}$ is a proper bubble function associated to an internal node.*

4 Numerical results

In this section, we present some numerical tests that confirm the expected rate of convergence of our schemes and show numerically that the discrete inf-sup condition holds true for the schemes that we have discussed.

We consider the case of a two-dimensional setting and choose $\Omega = [0,6] \times [0,6]$ and $\Omega_2 = [e, 1+\pi] \times [e, 1+\pi]$. This specific choice of the domains was previously used in [6] using the finite element $Q_1 - Q_1 - Q_1$ and was chosen in order to have the meshes not conforming at the interface. In addition, the right hand sides of the problem are fixed to be $f = 1$ and $f_2 = 1$.

Before we start let us describe how we treat numerically the coupling term $(\lambda_h, v_h|_{\Omega_2})_{\Omega_2}$ in Problem 2.3 where $\lambda_h \in \Lambda_h$ and $v_h \in V_h$. This term is represented as the L^2 scalar product in Ω_2. Evaluating this term requires the evaluation of the following integral:

$$\int_{\Omega_2} \phi_i \psi_j|_{\Omega_2} \, dx = \sum_{K \in \mathcal{T}_2} \int_K \phi_i \psi_j|_{\Omega_2} \, dx \tag{22}$$

where $\phi_i \; i = 1, \ldots, \dim(\Lambda_h)$ and $\psi_j \; j = 1, \ldots, \dim(V_h)$ are the basis functions that span Λ_h and V_h, respectively. Thanks to the choice of Λ_h, $\phi_i = 1$ on the element $K_i \in \mathcal{T}_2$ and vanishes elsewhere. Hence the integral in (22) reduces to the integral on the intersection between K_i with the support of ψ_j.

To simplify the idea, consider the 2D case and assume that the support of ϕ_i is the element $K_i \in \mathcal{T}_2$ colored with brown in Figure 6.A. We start by finding the geometric intersections of elements in $\mathcal{T}$ with K_i. This leads us to the introduction of a new mesh in Ω_2, that we denote by $\overline{\mathcal{T}}_2$ with the property that each element $\overline{K} \in \overline{\mathcal{T}}_2$ is contained in one element in $\mathcal{T}$ as in Figure 6.B. This new mesh is also a quadrilateral mesh but finer than $\mathcal{T}_2$. Therefore we have

$$\int_{\Omega_2} \phi_i \psi_j|_{\Omega_2} \, dx = \int_{K_i \cap \text{supp}(\psi_j)} \psi_j \, dx$$

where $K_i \cap \text{supp}(\psi_j)$ is the rectangle colored in red in Figure 6.C.

This approach will give us an exact evaluation of the scalar product since it takes into the account the exact region for which the two shape functions interact [3]. The procedure for adapting this approach is briefly summarized bellow:

- Choose the order of the quadrature rule depending on the degree of ψ_j.

- Find the corresponding quadrature points and weights in the reference element $\widehat{K}$. Denote by $\widehat{q_k}$ the kth quadrature point and by $\widehat{w_k}$ the associated quadrature weight.

- Map the quadrature points and weights to $\overline{K}$ where $\overline{K} = K_i \cap \text{supp}(\psi_j)$. So, we have $w_k = |\overline{K}| \, \widehat{w_k}$, and $\psi_j(q_k) = \widehat{\psi_j}(\widehat{q_k})$, see, for example, Figure 6.D.

- Evaluate the integral as follows:

$$\int_{\Omega_2} \phi_i \psi_j = \int_{\overline{K}} \psi_j = |\overline{K}| \int_{\widehat{K}} \widehat{\psi_j} = |\overline{K}| \sum_k \widehat{w_k} \widehat{\psi_j}(\widehat{q_k}) = \sum_k w_k \psi_j(q_k).$$
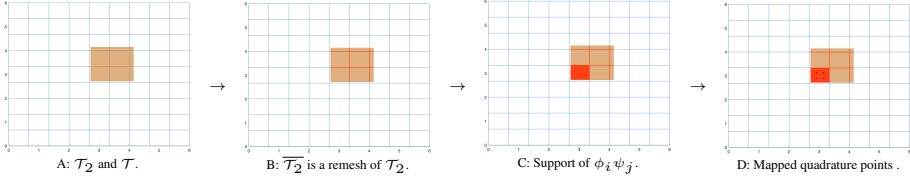
FIGURE 6: Intersection approach.

4.1 Numerical discrete inf-sup test

In this section, numerical tests on the discrete inf-sup bound of the proposed elements is presented to validate the theoretical proofs given in Section 3.

For the same reason explained in Section 3, it is enough to show that there exists a constant $\gamma_2 > 0$ such that the following inf-sup bound is satisfied:

$$\sup_{v_{2h} \in V_{2h}} \frac{(\mu_h, v_{2h})_{\Omega_2}}{\|v_{2h}\|_{V_2}} \geq \gamma_2 \|\mu_h\|_{\Lambda} \tag{23}$$

In order to estimate numerically the constant γ_2, we use the following standard procedure. Let N_1 and N_2 be the two matrices associated with the following norms:

$$\|v_2\|_{V_2}^2 = |v_2|_{V_2}^2 + \|v_2\|_{0,\Omega_2}^2 = v_2^T N_2 v_2 \qquad v_2 \in V_{2h}$$
$$\|\mu_h\|_{\Lambda}^2 \approx h_2 \|\mu_h\|_{0,\Omega_2}^2 = \mu_h^T (h_2 N_1) \mu_h \qquad \mu_h \in \Lambda_h$$

Arguing as in [16], the eigenvalue equation associated with this inf-sup condition is

$$(C_2) (h_2 N_1)^{-1} \left(C_2^T \right) v_2 = \sigma N_2 v_2 \tag{24}$$

where C_2 is the operator associated with the bilinear form $(\mu_h, v_{2h})_{\Omega_2}$. If the considered finite element satisfies the inf-sup condition, then, with increase refinements, the square root of the smallest eigenvalue σ_1 is bounded from below away from zero independently from the mesh sizes. This bound is the desired inf-sup bound.

The problem is solved in a sequence of five refinements. The results are plotted using logarithmic scaling. In Figure 7 we report the results of our test for the two elements presented in Section 3 together with the test for the element $Q_1 - Q_1 - P_0$, where we didn't add the bubble to the space V_{2h}.

It is clear that Element 1 and Element 2 are stable as the mesh is refined, that is the inf-sup constant doesn't degenerate, while the element without the bubble is not, that is, the inf-sup constant tends to zero as h goes to zero.
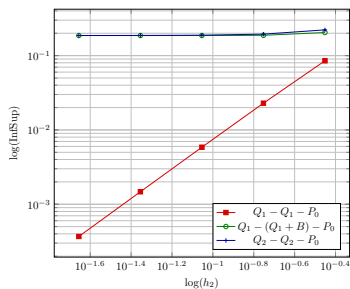
FIGURE 7: Numerical discrete Inf-Sup Test.

4.2 Rate of convergence

In this section, we show the numerical results of the rate of convergence of our proposed elements. We look at the performance by allowing the diffusion coefficients to vary as follow:

Case 1: $\beta < \beta_2$

Case 2: $\beta > \beta_2$

Clearly, **Case 2** is violating the elker condition constraint in Proposition 3.1. To obtain a better understanding of the performance, each case is tested with five different choices of the ratio between mesh-sizes $\frac{h}{h_2}$ denoted by r. In particular, r takes the values $\left\{\frac{1}{2}, \frac{1}{4}, 1, 2, 4\right\}$ over eight cycles of global uniform refinements and up to 400^2 grid points.

Case 1: In this case $\beta_2 - \beta > 0$, hence the elker condition is satisfied. We test two situations, $\beta = 1$, $\beta_2 = 10$ and $\beta = 1$, $\beta_2 = 10000$. In the first situation, when the difference is roughly small, all proposed elements perform more or less the same. They converge with optimal rate. We found that the L^2 error of u converges as $O(h)$ and the H^1 error as $O(h^{\frac{1}{2}})$. On the other hand, when the difference is larger, the elements converge optimally when the ratio r is less than or equal to 1. Figures 11, 13, 14, and 16 show a linear relation when the ratio r is small. As r increases, i.e. $\mathcal{T}$ is coarser than $\mathcal{T}_2$, we see more oscillations in the convergence plots. This could be related to the fact that the material with smaller diffusion coefficient requires a finer mesh since the solution changes rapidly there.

In general, those oscillations are not surprising. In one refinement step we might, by coincidence, have matching nodes in some places on Γ. However, in the next step, we could easily loose this matching at the interface. Nonetheless, errors were rather small and Tables 1 - 18 show that both the L^2 and H^1 errors are less than 10^{-2}. (n.o.e. refers to the number of elements used).

Case 2: In this case we have that $\beta_2 < \beta$. We, first, considered the case where the difference $\beta_2 - \beta$ is relatively small; namely $\beta = 10$, $\beta_2 = 1$. Surprisingly, we found that Element 2 is stable and provide the expected rate of convergence. As shown in Figure 15, the plots of the error for Element 2 are smooth independently from the ratio of

the mesh-sizes. Element 1, also, converged as expected when the ratio r is greater than one, as can be seen in Figure 12.

We extend the study of this case by increasing the difference between the coefficients and let $\beta_2 << \beta$. We tested the case when $\beta = 10000$ and $\beta_2 = 1$. In this particular situation, all elements did not converge. The results of **Case 2** suggest that the elker condition can be slightly weakened, perhaps under some constraints on the ratio between mesh sizes r.

To this end, we can say that by using a discontinuous Lagrange multiplier space, we were able to achieve similar results to what was obtained in [6] in the case when an L^2 scalar product is used to evaluate the duality term numerically. Results are similar in the sense that, in **Case 1** when $\beta = 1, \beta_2 = 10$, elements converges optimally and less oscillations appear as the ratio decreases. The situation when $\beta = 1, \beta_2 = 10000$ was not covered in their work. In **Case 2**, Element 1 shows an optimal convergence when the ratio is greater than 1 which is similar to what was found in [6]. However, Element 2 in this case outperforms their results and converges with optimal rate independently of the ratio.

We conclude this section by going back to the element $Q_1 - Q_1 - P_0$ due to its appeal coming from its easier implementation. Recall that, in Section 4.1, we showed numerically that this element does not pass the inf-sup test. However, Figure 8 shows that it converges with optimal rate in **Case 1** when the difference $\beta_2 - \beta$ is small enough. As the difference increases, the element convergences optimally when the ratio r is less than or equal to 1, as can be seen in Figure 10. Lastly, in **Case 2**, this element fails to converge as shown in Figure 9.

5   Conclusion

This paper proposes two elements for elliptic interface problems with jump coefficients. They were proven to be stable theoretically. The numerical results confirmed that the discrete inf-sup is bounded away from zero for the proposed elements. Moreover, the convergence rate is as expected. In the case of $\beta = 10$, $\beta_2 = 1$, the elements converge when the ratio r is greater than or equal to 1. On the other hand, in the case when $\beta_2 - \beta > 0$, the elements converge when the ratio r is less than or equal to 1. In all cases, Element 2 outperforms Element 1. These results extend those of [6] to the case where a discontinuous Lagrange multiplier is used. A potential future work would be to study the a posteriori error estimate for those schemes and use the results to apply some local refinements to control the overall error and reduce the computational cost by refining only where it is needed. Moreover, this work could be extended to a fluid structure interaction problem, which was the main motivation of our paper.
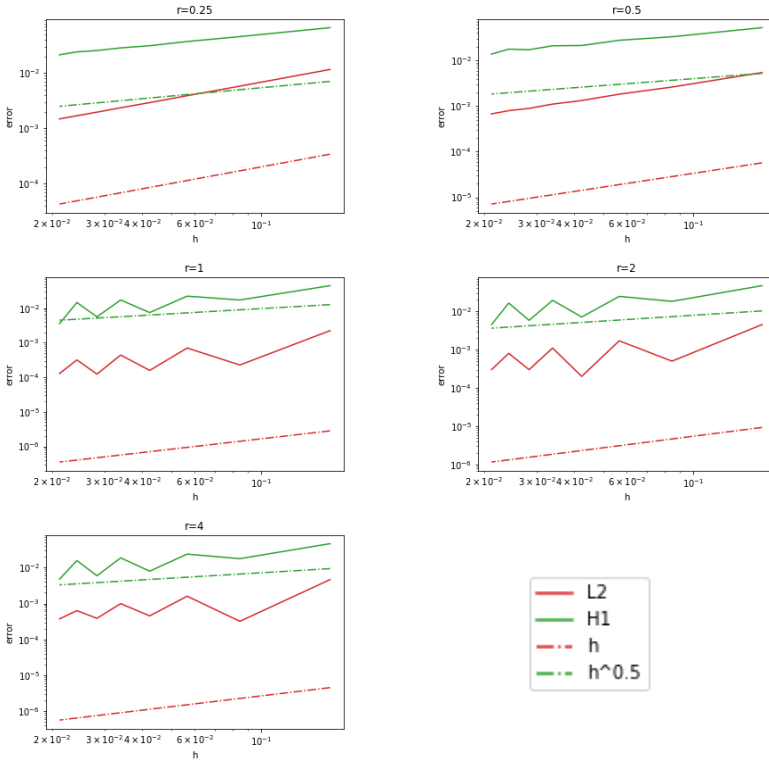
FIGURE 8: Convergence FDDLM $Q_1 - Q_1 - P_0$-FEM, u error, $\beta = 1$ $\beta_2 = 10$.

ref. step	n.o.e.	r=0.5	r=0.25	r=1	r=2	r=4
1	50^2	5.42×10^{-3}	1.17×10^{-2}	2.24×10^{-3}	4.50×10^{-3}	4.64×10^{-3}
2	100^2	2.61×10^{-3}	5.82×10^{-3}	2.27×10^{-4}	5.00×10^{-4}	3.20×10^{-4}
3	150^2	1.82×10^{-3}	3.91×10^{-3}	7.03×10^{-4}	1.70×10^{-3}	1.60×10^{-3}
4	200^2	1.32×10^{-3}	2.93×10^{-3}	1.58×10^{-4}	2.00×10^{-4}	4.53×10^{-4}
5	250^2	1.10×10^{-3}	2.36×10^{-3}	4.40×10^{-4}	1.10×10^{-3}	9.94×10^{-4}
6	300^2	8.89×10^{-4}	1.97×10^{-3}	1.24×10^{-4}	3.00×10^{-4}	3.88×10^{-4}
7	350^2	7.94×10^{-4}	1.70×10^{-3}	3.18×10^{-4}	8.00×10^{-4}	6.35×10^{-4}
8	400^2	6.74×10^{-4}	1.48×10^{-3}	1.28×10^{-4}	3.00×10^{-4}	3.74×10^{-4}

TABLE 1

FD/DLM $Q_1 - Q_1 - P_0$-FEM - L2 Error table for u, $\beta = 1$ $\beta_2 = 10$.

ref. step	n.o.e.	r=0.5	r=0.25	r=1	r=2	r=4
1	50^2	5.23×10^{-2}	6.67×10^{-2}	4.50×10^{-2}	4.67×10^{-2}	4.65×10^{-2}
2	100^2	3.30×10^{-2}	4.59×10^{-2}	1.73×10^{-2}	1.82×10^{-2}	1.78×10^{-2}
3	150^2	2.77×10^{-2}	3.74×10^{-2}	2.24×10^{-2}	2.45×10^{-2}	2.37×10^{-2}
4	200^2	2.13×10^{-2}	3.14×10^{-2}	7.48×10^{-3}	7.10×10^{-3}	7.97×10^{-3}
5	250^2	2.10×10^{-2}	2.87×10^{-2}	1.74×10^{-2}	1.94×10^{-2}	1.87×10^{-2}
6	300^2	1.72×10^{-2}	2.57×10^{-2}	5.63×10^{-3}	5.80×10^{-3}	5.93×10^{-3}
7	350^2	1.77×10^{-2}	2.43×10^{-2}	1.47×10^{-2}	1.64×10^{-2}	1.58×10^{-2}
8	400^2	1.38×10^{-2}	2.15×10^{-2}	3.57×10^{-3}	4.50×10^{-3}	4.77×10^{-3}

TABLE 2

FD/DLM $Q_1 - Q_1 - P_0$-FEM - H1 Error table for u, $\beta = 1$ $\beta_2 = 10$.

FIGURE 9: Convergence FDDLM $Q_1 - Q_1 - P_0$-FEM, u error, $\beta = 10 \; \beta_2 = 1$.

ref. step	n.o.e.	r=0.5	r=0.25	r=1	r=2	r=4
1	50^2	3.55×10^{-1}	1.46×10^{-1}	1.79×10^{-1}	4.25×10^{-1}	1.89×10^{-1}
2	100^2	6.86×10^{-2}	6.71×10^{1}	3.11×10^{-2}	2.25×10^{-1}	3.53×10^{-1}
3	150^2	3.58×10^{-2}	6.98×10^{-2}	1.06×10^{-2}	3.23×10^{-1}	4.27×10^{-1}
4	200^2	2.60×10^{0}	6.56×10^{-1}	1.51×10^{-2}	4.67×10^{-1}	3.26×10^{-1}
5	250^2	3.55×10^{-1}	4.58×10^{-2}	8.31×10^{-3}	9.33×10^{-1}	2.00×10^{-1}
6	300^2	2.37×10^{-1}	1.05×10^{-1}	2.39×10^{-3}	4.81×10^{-1}	2.40×10^{-1}
7	350^2	1.92×10^{-1}	1.81×10^{-1}	7.35×10^{-3}	5.21×10^{-1}	1.12×10^{-1}
8	400^2	1.52×10^{-1}	7.51×10^{-2}	4.94×10^{-3}	3.38×10^{-1}	5.09×10^{-1}

TABLE 3

FD/DLM $Q_1 - Q_1 - P_0$-FEM - L2 Error table for u, $\beta = 10 \; \beta_2 = 1$.

ref. step	n.o.e.	r=0.5	r=0.25	r=1	r=2	r=4
1	50^2	1.75×10^{0}	5.37×10^{-1}	1.78×10^{0}	6.24×10^{0}	2.48×10^{0}
2	100^2	7.47×10^{-1}	2.96×10^{2}	1.05×10^{0}	5.93×10^{0}	1.87×10^{0}
3	150^2	6.33×10^{-1}	5.77×10^{-1}	4.80×10^{-1}	6.08×10^{0}	6.86×10^{0}
4	200^2	5.39×10^{1}	7.13×10^{-1}	9.93×10^{-1}	2.63×10^{0}	7.55×10^{0}
5	250^2	1.29×10^{1}	5.97×10^{-1}	5.14×10^{-1}	3.67×10^{1}	6.10×10^{0}
6	300^2	1.05×10^{1}	1.81×10^{0}	2.72×10^{-1}	1.75×10^{1}	9.50×10^{-1}
7	350^2	8.12×10^{0}	6.21×10^{0}	5.15×10^{-1}	3.72×10^{1}	4.67×10^{0}
8	400^2	6.01×10^{0}	1.33×10^{0}	5.03×10^{-1}	1.81×10^{1}	5.54×10^{1}

TABLE 4

FD/DLM $Q_1 - Q_1 - P_0$-FEM - H1 Error table for u, $\beta = 10 \; \beta_2 = 1$.

FIGURE 10: Convergence FDDLM $Q_1 - Q_1 - P_0$-FEM, u error, $\beta = 1$ $\beta_2 = 10000$.

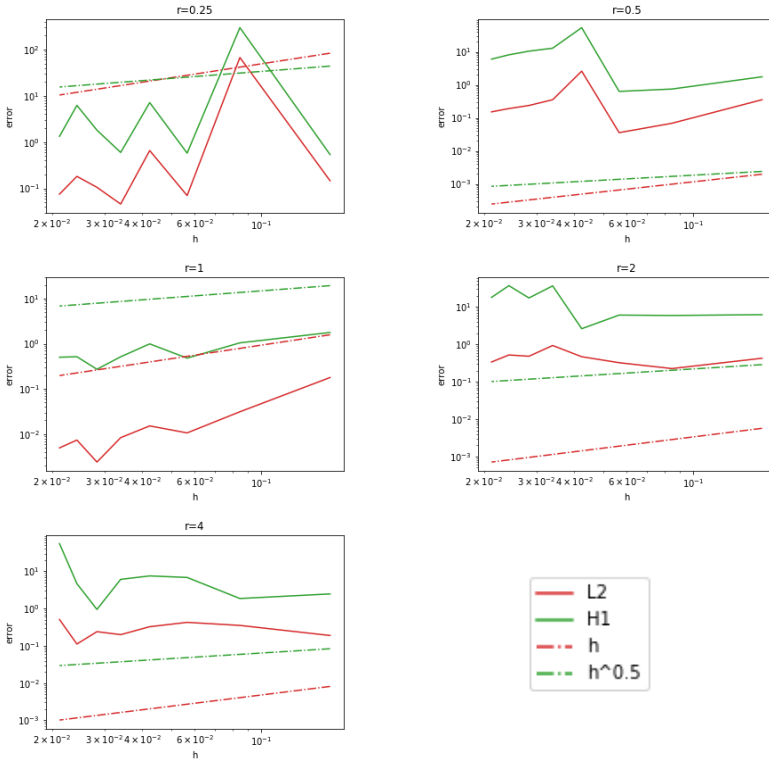| ref. step	n.o.e.	r=0.5	r=0.25	r=1	r=2	r=4
1	50^2	7.58×10^{-3}	1.58×10^{-2}	3.18×10^{-3}	9.56×10^{-3}	9.59×10^{-3}
2	100^2	3.76×10^{-3}	8.13×10^{-3}	3.52×10^{-4}	6.36×10^{-4}	1.55×10^{-3}
3	150^2	2.65×10^{-3}	5.55×10^{-3}	1.01×10^{-3}	2.53×10^{-3}	2.72×10^{-3}
4	200^2	1.95×10^{-3}	4.21×10^{-3}	2.65×10^{-4}	1.15×10^{-3}	2.89×10^{-3}
5	250^2	1.64×10^{-3}	3.42×10^{-3}	6.60×10^{-4}	1.48×10^{-3}	1.48×10^{-3}
6	300^2	1.33×10^{-3}	2.87×10^{-3}	1.87×10^{-4}	1.62×10^{-3}	2.31×10^{-3}
7	350^2	1.19×10^{-3}	2.49×10^{-3}	4.88×10^{-4}	1.07×10^{-3}	1.07×10^{-3}
8	400^2	1.01×10^{-3}	2.18×10^{-3}	2.07×10^{-4}	1.44×10^{-3}	1.64×10^{-3}

TABLE 5

FD/DLM $Q_1 - Q_1 - P_0$-FEM - L2 Error table for u, $\beta = 1$ $\beta_2 = 10000$.

ref. step	n.o.e.	r=0.5	r=0.25	r=1	r=2	r=4
1	50^2	6.09×10^{-2}	7.88×10^{-2}	5.15×10^{-2}	6.46×10^{-2}	6.47×10^{-2}
2	100^2	3.93×10^{-2}	5.53×10^{-2}	1.94×10^{-2}	2.12×10^{-2}	2.32×10^{-2}
3	150^2	3.35×10^{-2}	4.56×10^{-2}	2.65×10^{-2}	3.25×10^{-2}	3.32×10^{-2}
4	200^2	2.64×10^{-2}	3.88×10^{-2}	9.61×10^{-3}	1.52×10^{-2}	3.07×10^{-2}
5	250^2	2.57×10^{-2}	3.53×10^{-2}	2.11×10^{-2}	2.57×10^{-2}	2.57×10^{-2}
6	300^2	2.13×10^{-2}	3.19×10^{-2}	5.97×10^{-3}	2.25×10^{-2}	3.04×10^{-2}
7	350^2	2.20×10^{-2}	3.01×10^{-2}	1.81×10^{-2}	2.16×10^{-2}	2.16×10^{-2}
8	400^2	1.74×10^{-2}	2.68×10^{-2}	5.25×10^{-3}	2.33×10^{-2}	2.61×10^{-2}

TABLE 6

FD/DLM $Q_1 - Q_1 - P_0$-FEM - H1 Error table for u, $\beta = 1$ $\beta_2 = 10000$.

FIGURE 11: Convergence FDDLM $Q_1 - (Q_1 + B) - P_0$-FEM - u error,$\beta = 1$ $\beta_2 = 10$.

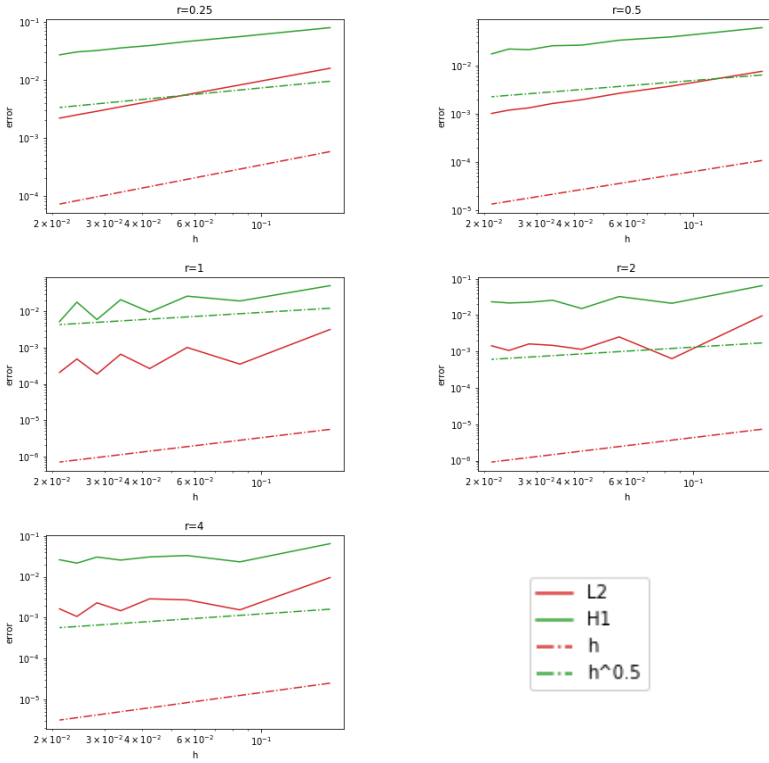| ref. step	n.o.e.	r=0.5	r=0.25	r=1	r=2	r=4
1	50^2	5.57×10^{-3}	1.19×10^{-2}	2.33×10^{-3}	3.51×10^{-3}	4.21×10^{-3}
2	100^2	2.69×10^{-3}	5.96×10^{-3}	3.66×10^{-4}	2.50×10^{-4}	2.51×10^{-4}
3	150^2	1.87×10^{-3}	4.00×10^{-3}	7.38×10^{-4}	1.15×10^{-3}	1.28×10^{-3}
4	200^2	1.37×10^{-3}	3.01×10^{-3}	2.24×10^{-4}	1.27×10^{-4}	1.75×10^{-4}
5	250^2	1.14×10^{-3}	2.42×10^{-3}	4.59×10^{-4}	6.98×10^{-4}	7.53×10^{-4}
6	300^2	9.18×10^{-4}	2.02×10^{-3}	1.63×10^{-4}	1.20×10^{-4}	6.76×10^{-5}
7	350^2	8.17×10^{-4}	1.74×10^{-3}	3.32×10^{-4}	4.85×10^{-4}	5.28×10^{-4}
8	400^2	6.95×10^{-4}	1.52×10^{-3}	1.55×10^{-4}	9.49×10^{-5}	4.01×10^{-5}

TABLE 7

FD/DLM $Q_1 - (Q_1 + B) - P_0$-FEM - L2 Error table for u, $\beta = 1$ $\beta_2 = 10$.

ref. step	n.o.e.	r=0.5	r=0.25	r=1	r=2	r=4
1	50^2	5.22×10^{-2}	6.66×10^{-2}	4.49×10^{-2}	4.39×10^{-2}	4.58×10^{-2}
2	100^2	3.30×10^{-2}	4.59×10^{-2}	1.75×10^{-2}	1.77×10^{-2}	1.77×10^{-2}
3	150^2	2.76×10^{-2}	3.74×10^{-2}	2.23×10^{-2}	2.26×10^{-2}	2.34×10^{-2}
4	200^2	2.12×10^{-2}	3.14×10^{-2}	7.59×10^{-3}	6.91×10^{-3}	7.42×10^{-3}
5	250^2	2.09×10^{-2}	2.87×10^{-2}	1.73×10^{-2}	1.79×10^{-2}	1.84×10^{-2}
6	300^2	1.72×10^{-2}	2.57×10^{-2}	5.71×10^{-3}	5.63×10^{-3}	5.68×10^{-3}
7	350^2	1.77×10^{-2}	2.43×10^{-2}	1.46×10^{-2}	1.52×10^{-2}	1.56×10^{-2}
8	400^2	1.38×10^{-2}	2.15×10^{-2}	3.55×10^{-3}	3.93×10^{-3}	4.13×10^{-3}

TABLE 8

FD/DLM $Q_1 - (Q_1 + B) - P_0$-FEM - H1 Error table for u, $\beta = 1$ $\beta_2 = 10$.

FIGURE 12: Convergence FDDLM $Q_1 - (Q_1 + B) - P_0$-FEM - u error,$\beta = 10$ $\beta_2 = 1$.

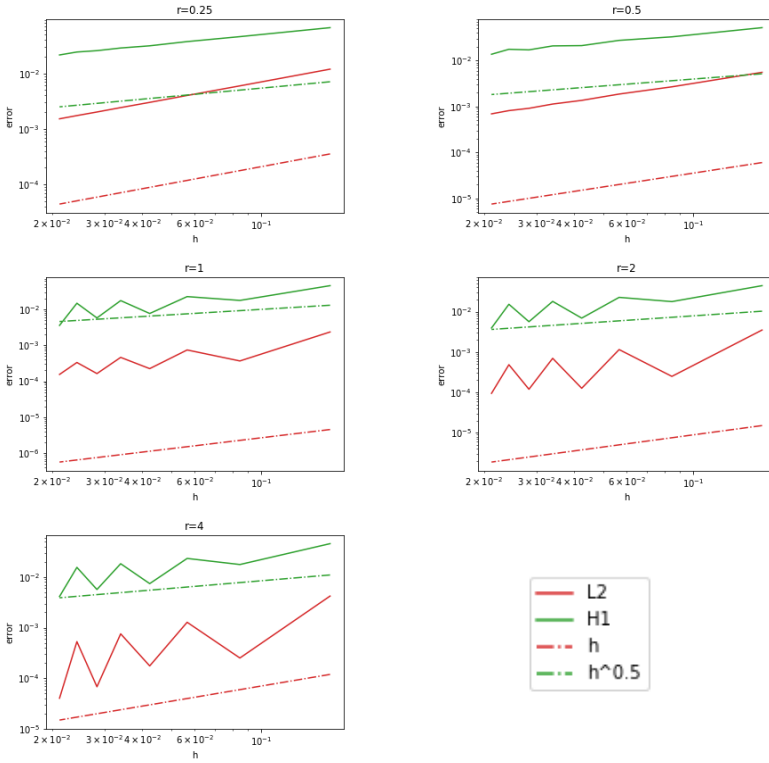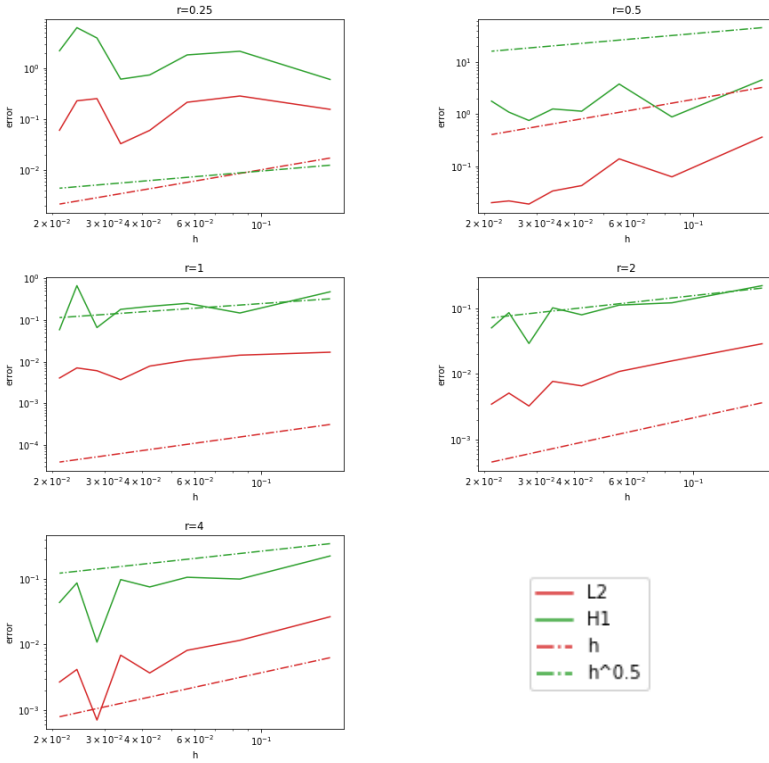| ref. step	n.o.e.	r=0.5	r=0.25	r=1	r=2	r=4
1	50^2	3.63×10^{-1}	1.56×10^{-1}	1.69×10^{-2}	2.88×10^{-2}	2.65×10^{-2}
2	100^2	6.26×10^{-2}	2.84×10^{-1}	1.44×10^{-2}	1.58×10^{-2}	1.16×10^{-2}
3	150^2	1.39×10^{-1}	2.14×10^{-1}	1.09×10^{-2}	1.09×10^{-2}	8.12×10^{-3}
4	200^2	4.26×10^{-2}	6.02×10^{-2}	7.86×10^{-3}	6.58×10^{-3}	3.66×10^{-3}
5	250^2	3.36×10^{-2}	3.29×10^{-2}	3.71×10^{-3}	7.70×10^{-3}	6.85×10^{-3}
6	300^2	1.88×10^{-2}	2.53×10^{-1}	6.08×10^{-3}	3.25×10^{-3}	6.97×10^{-4}
7	350^2	2.16×10^{-2}	2.29×10^{-1}	7.10×10^{-3}	5.11×10^{-3}	4.14×10^{-3}
8	400^2	2.00×10^{-2}	6.05×10^{-2}	4.06×10^{-3}	3.46×10^{-3}	2.66×10^{-3}

TABLE 9

FD/DLM $Q_1 - (Q_1 + B) - P_0$-FEM - L2 Error table for u,$\beta = 10$ $\beta_2 = 1$.

ref. step	n.o.e.	r=0.5	r=0.25	r=1	r=2	r=4
1	50^2	4.54×10^{0}	6.01×10^{-1}	4.79×10^{-1}	2.21×10^{-1}	2.25×10^{-1}
2	100^2	8.83×10^{-1}	2.15×10^{0}	1.48×10^{-1}	1.21×10^{-1}	9.99×10^{-2}
3	150^2	3.78×10^{0}	1.82×10^{0}	2.53×10^{-1}	1.12×10^{-1}	1.06×10^{-1}
4	200^2	1.14×10^{0}	7.37×10^{-1}	2.14×10^{-1}	7.95×10^{-2}	7.57×10^{-2}
5	250^2	1.26×10^{0}	6.09×10^{-1}	1.81×10^{-1}	1.02×10^{-1}	9.81×10^{-2}
6	300^2	7.55×10^{-1}	3.91×10^{0}	6.63×10^{-2}	2.91×10^{-2}	1.08×10^{-2}
7	350^2	1.09×10^{0}	6.24×10^{0}	6.73×10^{-1}	8.58×10^{-2}	8.72×10^{-2}
8	400^2	1.77×10^{0}	2.20×10^{0}	5.88×10^{-2}	5.04×10^{-2}	4.39×10^{-2}

TABLE 10

FD/DLM $Q_1 - (Q_1 + B) - P_0$-FEM - H1 Error table for u, $\beta = 10$ $\beta_2 = 1$.

FIGURE 13: Convergence FDDLM $Q_1-(Q_1+B)-P_0$-FEM - u error,$\beta = 1$ $\beta_2 = 10000$.

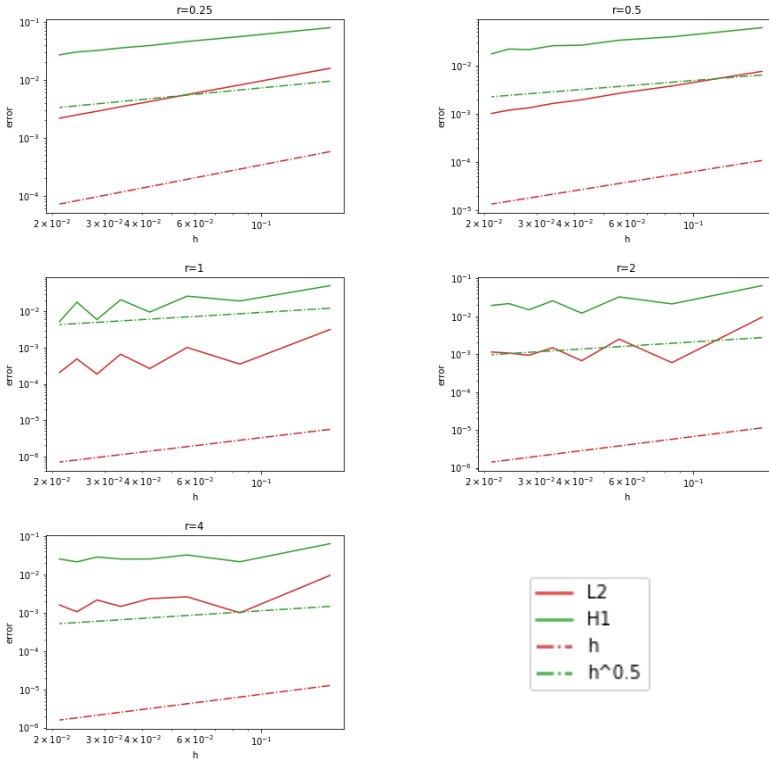| ref. step	n.o.e.	r=0.5	r=0.25	r=1	r=2	r=4
1	50^2	7.58×10^{-3}	1.58×10^{-2}	3.18×10^{-3}	9.48×10^{-3}	9.58×10^{-3}
2	100^2	3.76×10^{-3}	8.13×10^{-3}	3.52×10^{-4}	5.95×10^{-4}	1.00×10^{-3}
3	150^2	2.65×10^{-3}	5.55×10^{-3}	1.01×10^{-3}	2.49×10^{-3}	2.63×10^{-3}
4	200^2	1.95×10^{-3}	4.21×10^{-3}	2.65×10^{-4}	6.70×10^{-4}	2.36×10^{-3}
5	250^2	1.64×10^{-3}	3.42×10^{-3}	6.60×10^{-4}	1.48×10^{-3}	1.48×10^{-3}
6	300^2	1.33×10^{-3}	2.87×10^{-3}	1.87×10^{-4}	9.35×10^{-4}	2.18×10^{-3}
7	350^2	1.19×10^{-3}	2.49×10^{-3}	4.88×10^{-4}	1.07×10^{-3}	1.07×10^{-3}
8	400^2	1.01×10^{-3}	2.18×10^{-3}	2.07×10^{-4}	1.14×10^{-3}	1.61×10^{-3}

TABLE 11

FD/DLM $Q_1 - (Q_1 + B) - P_0$-FEM - L2 Error table for u,$\beta = 1$ $\beta_2 = 10000$.

ref. step	n.o.e.	r=0.5	r=0.25	r=1	r=2	r=4
1	50^2	6.09×10^{-2}	7.88×10^{-2}	5.15×10^{-2}	6.42×10^{-2}	6.47×10^{-2}
2	100^2	3.93×10^{-2}	5.53×10^{-2}	1.94×10^{-2}	2.12×10^{-2}	2.17×10^{-2}
3	150^2	3.35×10^{-2}	4.56×10^{-2}	2.65×10^{-2}	3.24×10^{-2}	3.28×10^{-2}
4	200^2	2.64×10^{-2}	3.88×10^{-2}	9.61×10^{-3}	1.21×10^{-2}	2.57×10^{-2}
5	250^2	2.57×10^{-2}	3.53×10^{-2}	2.11×10^{-2}	2.57×10^{-2}	2.57×10^{-2}
6	300^2	2.13×10^{-2}	3.19×10^{-2}	5.97×10^{-3}	1.48×10^{-2}	2.89×10^{-2}
7	350^2	2.20×10^{-2}	3.01×10^{-2}	1.81×10^{-2}	2.16×10^{-2}	2.16×10^{-2}
8	400^2	1.74×10^{-2}	2.68×10^{-2}	5.25×10^{-3}	1.92×10^{-2}	2.56×10^{-2}

TABLE 12

FD/DLM $Q_1 - (Q_1 + B) - P_0$-FEM - H1 Error table for u, $\beta = 1$ $\beta_2 = 10000$.

FIGURE 14: Convergence FDDLM $Q_2 - Q_2 - P_0$-FEM -u error, $\beta = 1$ $\beta_2 = 10$.

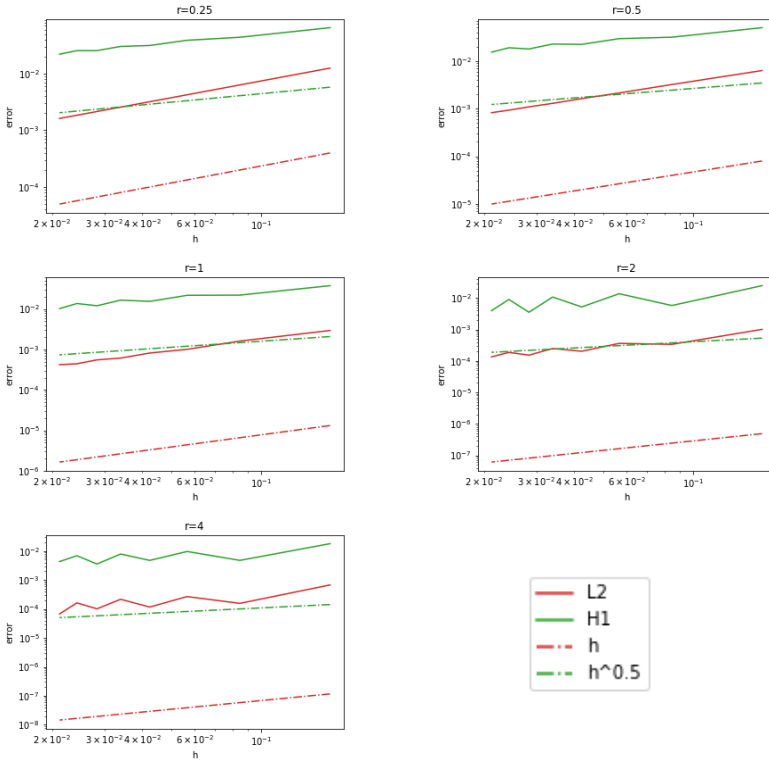| ref. step	n.o.e.	r=0.5	r=0.25	r=1	r=2	r=4
1	50^2	6.28×10^{-3}	1.26×10^{-2}	2.94×10^{-3}	1.01×10^{-3}	6.73×10^{-4}
2	100^2	3.19×10^{-3}	6.33×10^{-3}	1.61×10^{-3}	3.37×10^{-4}	1.56×10^{-4}
3	150^2	2.13×10^{-3}	4.24×10^{-3}	1.01×10^{-3}	3.62×10^{-4}	2.67×10^{-4}
4	200^2	1.62×10^{-3}	3.20×10^{-3}	8.15×10^{-4}	2.03×10^{-4}	1.16×10^{-4}
5	250^2	1.29×10^{-3}	2.56×10^{-3}	6.11×10^{-4}	2.48×10^{-4}	2.15×10^{-4}
6	300^2	1.09×10^{-3}	2.15×10^{-3}	5.51×10^{-4}	1.53×10^{-4}	1.01×10^{-4}
7	350^2	9.26×10^{-4}	1.84×10^{-3}	4.42×10^{-4}	1.87×10^{-4}	1.62×10^{-4}
8	400^2	8.20×10^{-4}	1.62×10^{-3}	4.20×10^{-4}	1.35×10^{-4}	6.71×10^{-5}

TABLE 13

FD/DLM $Q_2 - Q_2 - P_0$-FEM - L2 Error table for u, $\beta = 1$ $\beta_2 = 10$.

ref. step	n.o.e.	r=0.5	r=0.25	r=1	r=2	r=4
1	50^2	4.98×10^{-2}	6.51×10^{-2}	3.77×10^{-2}	2.48×10^{-2}	1.79×10^{-2}
2	100^2	3.14×10^{-2}	4.40×10^{-2}	2.20×10^{-2}	5.79×10^{-3}	4.74×10^{-3}
3	150^2	2.93×10^{-2}	3.90×10^{-2}	2.18×10^{-2}	1.37×10^{-2}	9.62×10^{-3}
4	200^2	2.22×10^{-2}	3.15×10^{-2}	1.54×10^{-2}	5.22×10^{-3}	4.73×10^{-3}
5	250^2	2.26×10^{-2}	3.03×10^{-2}	1.66×10^{-2}	1.08×10^{-2}	7.86×10^{-3}
6	300^2	1.78×10^{-2}	2.56×10^{-2}	1.20×10^{-2}	3.53×10^{-3}	3.55×10^{-3}
7	350^2	1.89×10^{-2}	2.55×10^{-2}	1.37×10^{-2}	9.01×10^{-3}	6.88×10^{-3}
8	400^2	1.52×10^{-2}	2.21×10^{-2}	1.02×10^{-2}	3.96×10^{-3}	4.30×10^{-3}

TABLE 14

FD/DLM $Q_2 - Q_2 - P_0$-FEM - H1 Error table for u, $\beta = 1$ $\beta_2 = 10$.

FIGURE 15: Convergence FDDLM $Q_2 - Q_2 - P_0$-FEM -u error, $\beta = 10$ $\beta_2 = 1$.

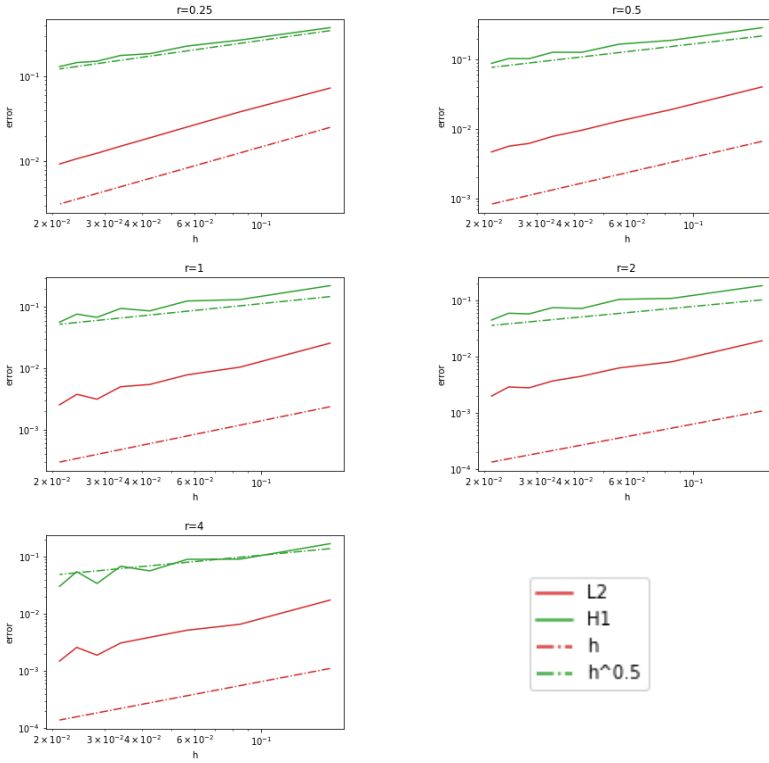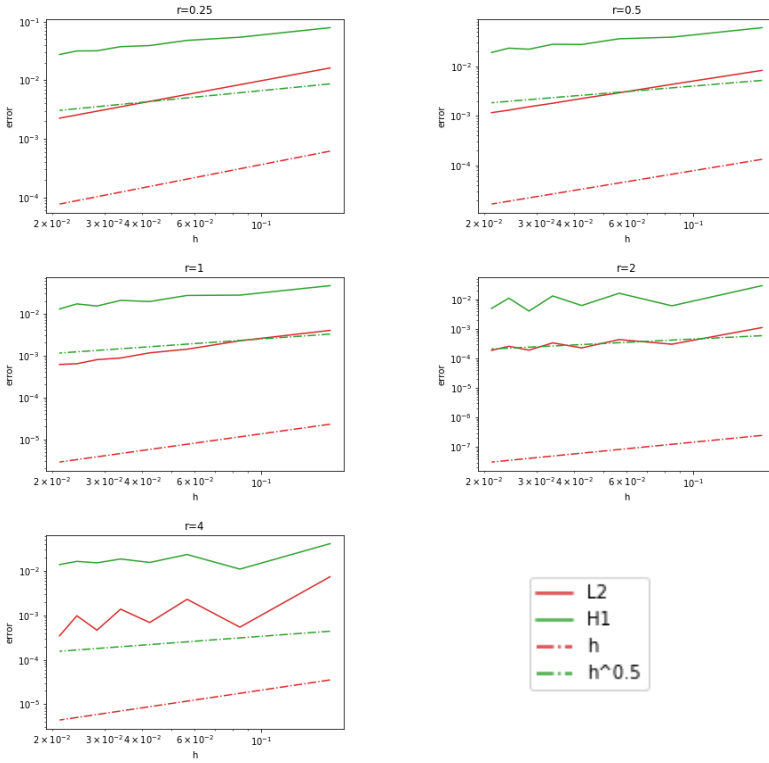| ref. step	n.o.e.	r=0.5	r=0.25	r=1	r=2	r=4
1	50^2	4.04×10^{-2}	7.30×10^{-2}	2.57×10^{-2}	1.91×10^{-2}	1.75×10^{-2}
2	100^2	1.92×10^{-2}	3.83×10^{-2}	1.04×10^{-2}	8.10×10^{-3}	6.60×10^{-3}
3	150^2	1.30×10^{-2}	2.54×10^{-2}	7.83×10^{-3}	6.30×10^{-3}	5.20×10^{-3}
4	200^2	9.58×10^{-3}	1.89×10^{-2}	5.45×10^{-3}	4.50×10^{-3}	3.90×10^{-3}
5	250^2	7.84×10^{-3}	1.51×10^{-2}	5.01×10^{-3}	3.70×10^{-3}	3.10×10^{-3}
6	300^2	6.19×10^{-3}	1.25×10^{-2}	3.13×10^{-3}	2.80×10^{-3}	1.90×10^{-3}
7	350^2	5.66×10^{-3}	1.07×10^{-2}	3.77×10^{-3}	2.90×10^{-3}	2.60×10^{-3}
8	400^2	4.67×10^{-3}	9.31×10^{-3}	2.54×10^{-3}	2.00×10^{-3}	1.50×10^{-3}

TABLE 15

FD/DLM $Q_2 - Q_2 - P_0$-FEM - L2 Error table for u, $\beta = 10$ $\beta_2 = 1$.

ref. step	n.o.e.	r=0.5	r=0.25	r=1	r=2	r=4
1	50^2	2.88×10^{-1}	3.76×10^{-1}	2.23×10^{-1}	1.81×10^{-1}	1.70×10^{-1}
2	100^2	1.89×10^{-1}	2.68×10^{-1}	1.32×10^{-1}	1.08×10^{-1}	9.11×10^{-2}
3	150^2	1.66×10^{-1}	2.28×10^{-1}	1.26×10^{-1}	1.03×10^{-1}	9.05×10^{-2}
4	200^2	1.27×10^{-1}	1.85×10^{-1}	8.65×10^{-2}	7.13×10^{-2}	5.68×10^{-2}
5	250^2	1.27×10^{-1}	1.77×10^{-1}	9.50×10^{-2}	7.37×10^{-2}	6.84×10^{-2}
6	300^2	1.03×10^{-1}	1.51×10^{-1}	6.79×10^{-2}	5.71×10^{-2}	3.42×10^{-2}
7	350^2	1.03×10^{-1}	1.46×10^{-1}	7.67×10^{-2}	5.87×10^{-2}	5.50×10^{-2}
8	400^2	8.83×10^{-2}	1.31×10^{-1}	5.67×10^{-2}	4.44×10^{-2}	3.04×10^{-2}

TABLE 16

FD/DLM $Q_2 - Q_2 - P_0$-FEM - H1 Error table for u, $\beta = 10$ $\beta_2 = 1$.

FIGURE 16: Convergence FDDLM $Q_2 - Q_2 - P_0$-FEM -u error, $\beta = 1$ $\beta_2 = 10000$.

ref. step	n.o.e.	r=0.5	r=0.25	r=1	r=2	r=4
1	50^2	8.32×10^{-3}	1.62×10^{-2}	3.96×10^{-3}	1.12×10^{-3}	7.42×10^{-3}
2	100^2	4.35×10^{-3}	8.40×10^{-3}	2.24×10^{-3}	3.05×10^{-4}	5.44×10^{-4}
3	150^2	2.93×10^{-3}	5.72×10^{-3}	1.41×10^{-3}	4.38×10^{-4}	2.31×10^{-3}
4	200^2	2.25×10^{-3}	4.35×10^{-3}	1.15×10^{-3}	2.29×10^{-4}	6.91×10^{-4}
5	250^2	1.80×10^{-3}	3.52×10^{-3}	8.69×10^{-4}	3.39×10^{-4}	1.38×10^{-3}
6	300^2	1.53×10^{-3}	2.96×10^{-3}	7.94×10^{-4}	1.92×10^{-4}	4.66×10^{-4}
7	350^2	1.31×10^{-3}	2.56×10^{-3}	6.33×10^{-4}	2.60×10^{-4}	9.83×10^{-4}
8	400^2	1.17×10^{-3}	2.25×10^{-3}	6.10×10^{-4}	1.88×10^{-4}	3.47×10^{-4}

TABLE 17

FD/DLM $Q_2 - Q_2 - P_0$-FEM - L2 Error table for u, $\beta = 1$ $\beta_2 = 10000$.

ref. step	n.o.e.	r=0.5	r=0.25	r=1	r=2	r=4
1	50^2	6.06×10^{-2}	7.89×10^{-2}	4.62×10^{-2}	2.94×10^{-2}	4.12×10^{-2}
2	100^2	3.90×10^{-2}	5.42×10^{-2}	2.75×10^{-2}	6.10×10^{-3}	1.10×10^{-2}
3	150^2	3.61×10^{-2}	4.78×10^{-2}	2.70×10^{-2}	1.62×10^{-2}	2.35×10^{-2}
4	200^2	2.78×10^{-2}	3.91×10^{-2}	1.93×10^{-2}	6.23×10^{-3}	1.56×10^{-2}
5	250^2	2.80×10^{-2}	3.74×10^{-2}	2.06×10^{-2}	1.32×10^{-2}	1.86×10^{-2}
6	300^2	2.23×10^{-2}	3.18×10^{-2}	1.51×10^{-2}	4.05×10^{-3}	1.53×10^{-2}
7	350^2	2.34×10^{-2}	3.16×10^{-2}	1.70×10^{-2}	1.11×10^{-2}	1.65×10^{-2}
8	400^2	1.91×10^{-2}	2.75×10^{-2}	1.28×10^{-2}	4.98×10^{-3}	1.39×10^{-2}

TABLE 18

FD/DLM $Q_2 - Q_2 - P_0$-FEM - H1 Error table for u, $\beta = 1$ $\beta_2 = 10000$.

References

[1] Auricchio, F., Boffi, D., Gastaldi, L., Lefieux, A., and Reali, A. (2015). On a fictitious domain method with distributed Lagrange multiplier for interface problems. *Applied Numerical Mathematics*, 95:36–50.

[2] Boffi, D., Brezzi, F., and Fortin, M. (2013). *Mixed finite element methods and applications*, volume 44. Springer.

[3] Boffi, D., Credali, F., and Gastaldi, L. (2022). On the interface matrix for fluid-structure interaction problems with fictitious domain approach. *arXiv preprint arXiv:2205.13350*.

[4] Boffi, D. and Gastaldi, L. (2003). A finite element approach for the immersed boundary method. *Computers & structures*, 81(8-11):491–501.

[5] Boffi, D. and Gastaldi, L. (2021). On the existence and the uniqueness of the solution to a fluid-structure interaction problem. *Journal of Differential Equations*, 279:136–161.

[6] Boffi, D., Gastaldi, L., and Ruggeri, M. (2014). Mixed formulation for interface problems with distributed Lagrange multiplier. *Computers & Mathematics with Applications*, 68(12):2151–2166.

[7] Brezzi, F., Boffi, D., Demkowicz, L., Durán, R., Falk, R., and Fortin, M. (2008). Mixed finite elements, compatibility conditions, and applications. *Springer*, 2:4–2.

[8] Chen, L., Wei, H., and Wen, M. (2017). An interface-fitted mesh generator and virtual element methods for elliptic interface problems. *Journal of Computational Physics*, 334:327–348.

[9] Ern, A. and Guermond, J.-L. (2017). Finite element quasi-interpolation and best approximation. *ESAIM: M2AN*, 51:1367–1385.

[10] Gerstenberger, A. and Wall, W. (2008). An extended finite element method/Lagrange multiplier based approach for fluid–structure interaction. *Computer Methods in Applied Mechanics and Engineering*, 197(19-20):1699–1714.

[11] Glowinski, R., Pan, T.-W., and Periaux, J. (1994). A fictitious domain method for Dirichlet problem and applications. *Computer Methods in Applied Mechanics and Engineering*, 111(3-4):283–303.

[12] Hansbo, A. and Hansbo, P. (2002). An unfitted finite element method, based on nitsche's method, for elliptic interface problems. *Computer methods in applied mechanics and engineering*, 191(47-48):5537–5552.

[13] Hansbo, P., Lovadina, C., Perugia, I., and Sangalli, G. (2005). A Lagrange multiplier method for the finite element solution of elliptic interface problems using non-matching meshes. *Numerische Mathematik*, 100(1):91–115.

[14] Hou, T., Wu, X.-H., and Cai, Z. (1999). Convergence of a multiscale finite element method for elliptic problems with rapidly oscillating coefficients. *Mathematics of computation*, 68(227):913–943.

[15] LeVeque, R. and Li, Z. (1994). The immersed interface method for elliptic equations with discontinuous coefficients and singular sources. *SIAM Journal on Numerical Analysis*, 31(4):1019–1044.

[16] Malkus, D. (1981). Eigenproblems associated with the discrete LBB condition for incompressible finite elements. *International Journal of Engineering Science*, 19(10):1299–1310.

[17] Nicaise, S. (1993). *Polygonal interface problems*, volume 39. Peter Lang, Frankfurt am Main.

[18] Peskin, C. (1972). Flow patterns around heart valves: a numerical method. *Journal of computational physics*, 10(2):252–271.

[19] Yu, Z. (2005). A DLM/FD method for fluid/flexible-body interactions. *Journal of computational physics*, 207(1):1–27.